A tradeoff between robustness to environmental fluctuations and speed of evolution

Max Schmid[1], Maria Paniw[1,2], Maarten Postuma[1,3], Arpat Ozgul[1], & Frédéric Guillaume[1]*

[1] Department of Evolutionary Biology and Environmental Studies, University of Zurich, Winterthurerstrasse 190, CH-8057, Zurich, Switzerland
[2] Ecological and Forestry Applications Research Centre (CREAF), Campus de Bellaterra (UAB) Edifici C, ES-08193 Cerdanyola del Vallès, Spain
[3] Plant Ecology and Nature Conservation Group, Wageningen University, 6700 AA Wageningen, the Netherlands

* corresponding author, email: frederic.guillaume@ieu.uzh.ch

Abstract

Organisms must cope with both short- and long-term environmental changes to persist. In this study we investigated theoretically if life histories trade off between their robustness to short-term environmental perturbations and their ability to evolve directional trait changes. By the use of mathematical models and stochastic individual-based simulations we could confirm the tradeoff, at least for comparisons between standardized life histories. Offspring dormancy and high adult survival allowed to maintain large population sizes when confronted with interannual environmental fluctuations while depressing the speed of evolution with ongoing environmental change. Instead, precocious offspring maturation and short-living adults promoted evolvability while lowering robustness. This tradeoff had immediate consequences for extinction dynamics in variable environments. High evolvability allowed to cope best with long-lasting gradual environmental change, but came at the expense of more pronounced population declines from environmental variability and during the initial phase of environmental change.

Introduction

Environmental conditions are rarely constant but fluctuate between years and average conditions change gradually over time, and both dynamics pose a considerable challenge for species (Bürger and Lynch, 1995; Boyce et al., 2006; Van De Pol et al., 2010; Vázquez et al., 2015). Average global temperatures change successively in the course of long-term glacial cycles or during ongoing anthropogenic climate change, but also vary on shorter time scales, for instance with variations between years (Stocker et al., 2013; Ummenhofer and Meehl, 2017). Given that the environmental tolerance of all species is finite, the exposure to environmental conditions different from optimal conditions can result in higher mortality, lower recruitment, and population declines. A dynamic environment thus demands species to constantly adapt and adjust. While species evolved a diverse set of strategies to cope with a varying environment (Parmesan, 2006; Aitken et al., 2008; Bell and Gonzalez, 2009; Doak and Morris, 2010; Duputié et al., 2015; Cayuela et al., 2017; McDonald et al., 2017), all these strategies are constrained and might not be adaptive with every kind of temporal change. Life-history strategies affect both, the robustness against interannual environmental fluctuations (Caswell, 2001; Boyce et al., 2006; Morris et al., 2008; Tuljapurkar et al., 2009) and the speed of genetic evolution in response to long-term directional change (Barfield et al., 2011; Orive et al., 2017). However, the suitability of life histories to cope with one kind of environmental variability might come at a cost to cope with another kind of dynamic environment.

A species' life history could help to buffer against short-term environmental variability by controlling the proportion of individuals exposed to environmental extremes, by shaping the effect of environmental variability on population growth rates, and by influencing the speed of population recovery (Tuljapurkar, 1982; Lande and Orzack, 1988; Tuljapurkar, 1990; Caswell, 2001; Morris et al., 2008). Stochasticity in vital rates from environmental variability has been shown to reduce the geometric mean fitness of populations, to depress population sizes, and thereby to increase extinction risk (Engen et al., 2005; Sæther et al., 2013; Chevin et al., 2017). How severely environmental variability feeds back on population viability depends on the species' life cycle, especially on its position along the fast-slow continuum and its reproductive strategy (Salguero-Gómez et al., 2017). Morris et al. (2008) found a relation between the life expectancy of 36 plant and animal species and their sensitivity to environmentally driven variation in vital rates.

Life histories with long generation times did experience less pronounced demographic consequences from stochasticity in vital rates than short-lived species (see also Dalgleish et al., 2010; Sæther et al., 2013). The temporal patterning of fluctuations is also crucial for population dynamics (Engen et al., 2013). The growth rates of fast life histories were shown to be more sensitive to temporal autocorrelation in environmental fluctuations than slow life histories (Paniw et al., 2017). A life history's robustness against environmental fluctuations further varies with the presence or absence of highly tolerant age or stage classes, which is often associated with long generation times. For instance plant seeds or adult trees often exhibit a high tolerance against extreme temperatures or drought events and can overcome detrimental conditions much better than seedlings or juvenile plants (Petit and Hampe, 2006; Buoro and Carlson, 2014). Delayed maturation (e.g., by seed or egg dormancy) then can allow to cope with temporally fluctuating environments by "dispersal through time" (Evans and Dennehy, 2005; Buoro and Carlson, 2014). As a consequence, a species' life history is a critical factor for population dynamics with interannual environmental variation (Tuljapurkar, 1990; Charlesworth, 1994; Morris et al., 2008).

Life-history strategies also shape the rate of trait evolution by their effect on changes in the genetic composition of a population, the number of individuals exposed to selection, and the genetic diversity maintained within a population (Lande, 1982; Ellner and Hairston, 1994; Metcalf and Pavard, 2007; Barfield et al., 2011; Orive et al., 2017). In quantitative genetics, the response to selection depends on the selection gradient ($\beta(z)$), the heritability of the trait (h^2), and its additive genetic variance (G_2) (Via and Lande, 1985; Falconer and Mackay, 1996). But the rate of evolution further depends in many ways on the life history of a species (Templeton and Levin, 1979; Lande, 1982; Barfield et al., 2011; Orive et al., 2017). The generation time of a species, which affects the pace of life, is an indicator for the average time from birth to reproduction and thus for the turnover rate of the gene pool. The faster selection can translate into changes of the gene pool, that is the lower the generation time, the faster is the evolutionary response to directional environmental change per unit of time (Vander Wal et al., 2013; Carlson et al., 2014; Orive et al., 2017). With life stages highly tolerant to environmental variation, life-history strategies further control the proportion of individuals exposed to the environment. Those genotypes "hidden" in the seedbank or in highly tolerant adult stages are not under selection and thereby delay genetic changes at the population level (Templeton and Levin, 1979; Hairston and De Stasio Jr., 1988; Barfield et al.,

2011; Orive et al., 2017). Similarly, the reproductive mode of a life history as whether and how long adults survive and reproduce (semelparity vs iteroparity) can slow down or accelerate evolution (Orive et al., 2017). Life-history strategies have therefore large effects on the speed of evolution, and thus on the success of evolutionary rescue.

Combining these previous findings it is reasonable to expect a tradeoff between a life history's effect on the sensitivity to environmental fluctuations (robustness) and its effect on the rate of directional trait evolution (evolvability). The more individuals get exposed to selection and the faster selection translates into changes of the gene pool, the faster evolution should proceed but the more severely a population might suffer from environmental perturbations. We are aware that the terms 'robustness' and 'evolvability' have been used in evolutionary biology since a long time, even though in a different context (Pigliucci, 2008; Brown, 2014; Crother and Murray, 2019). We generally refer to evolvability as the ability to evolve, similar to Hansen et al. (2019), but with focus on the effect of life-history strategies on this capability. While robustness has been used repeatedly with regard to mutational robustness (e.g., see de Visser et al., 2003), we apply this term to describe the capacity of life-history strategies to withstand interannual environmental fluctuations. A tradeoff between robustness and evolvability in this sense would indicate that a life-history strategy could not allow to evolve fast and resist environmental variation simultaneously. The existence of such a tradeoff between evolvability and robustness has been further indicated by the results of Hairston and De Stasio Jr. (1988) and Templeton and Levin (1979) who found that the presence of a seed bank slowed down the rate of phenotypic trait evolution. Similarly, Orive et al. (2017) found that elevated iteroparity (with adults shielded from selection) supported population recovery after a sudden step change in the environment, but made a successful evolutionary rescue with gradual environmental change less likely. However, a systematic test for a tradeoff between evolvability and robustness with regard to life-history strategies has not been conducted so far.

While a similar tradeoff between robustness and evolvability has been hypothesized before for phenotypes, there it could be overcome via indirect effects on genetic diversity (Ancel, 2000; de Visser et al., 2003; Sumedha et al., 2007; Wagner, 2008; Mayer and Hansen, 2017; Payne and Wagner, 2018). In some situations a higher robustness allowed to accumulate larger levels of genetic diversity, such that more robust systems could also evolve faster (Wagner, 2008). For life-history strategies, a similar process might

allow to combine high robustness to environmental fluctuations with fast trait evolution. Life histories with overlapping generations were suggested to harbour higher levels of additive genetic variance in a variable environment than life histories with non-overlapping generations, a process known as the genetic storage effect (Ellner and Hairston, 1994; Sasaki and Ellner, 1997; Svardal et al., 2015). The existence of highly tolerant life-history stages then could allow to maintain genetic diversity within populations when genetic variants could be shielded from detrimental environmental events in seed banks or in robust adult stages. Given that the likelihood of a successful evolutionary rescue increases with the extent of standing genetic variation (Carlson et al., 2014), life histories with highly robust life stages might be able to accumulate higher levels of genetic variance, and thus also evolve faster (Yamamichi et al., 2019).

Here we tested theoretically if a tradeoff between a life history's robustness against environmental fluctuations and rate of trait evolution exists, or if it could be overcome by the genetic storage effect. We used individual-based simulations and mathematical models to study the effect of life-history parameters on the speed of quantitative genetic evolution and the equilibrium population sizes in face of environmental variability. We modeled single populations with 3-stage life cycles (offspring, juveniles, adults) that reached a carrying capacity from negative density dependent survival. Only juveniles were under selection such that only their survival varied with the environment, while offspring and adults very highly tolerant. We then exposed the population to interannual fluctuations in the environment together with gradual changes of the average condition. We used individual-based simulations in addition to the mathematical models to account for demographic and genetic stochasticity and evolving additive genetic variances. The simulations further allowed us to study the effect of robustness and evolvability on extinction probabilities with regard to different degrees of interannual variation and environmental change.

Methods

General

We modeled a single hermaphroditic species with three life stages (offspring (n_1), juveniles (n_2), and adults (n_3)) forming a single panmictic population (i.e. with random mating between adult individuals).

The population reached an equilibrium population size ($\hat{n}_t$) from intra-specific density regulation. We assumed that only the survival of juveniles was negatively affected by the environment, while individuals in the offspring and adult stage were shielded from the environment. Selection acted on juveniles only, either because the focal trait was only expressed in the juvenile stage (e.g., growth), offspring and adult individuals had a much higher environmental tolerance (e.g., frost or drought tolerance), or dwelled in much more stable habitats (e.g., Petit and Hampe, 2006; Van De Pol et al., 2010; Marshall et al., 2016). As a consequence of the negative density dependence, a reduction in juvenile survival from environmental variability or directional selection did not necessarily lead to a deterministic population decline but resulted in a lower equilibrium population size. Then, negative effects of detrimental environmental conditions were partially compensated by relaxed intra-specific competition (Fig. 1d,e).

We modeled life histories with overlapping generations as three-stage models such that offspring and adult individuals could stay within their stage over subsequent years (Fig. 1a). In order to model a life history with non-overlapping generations, we modeled a biennial two-stage life cycle with offspring individuals maturing immediately to the juvenile stage, and adults reproducing only once before they died (Fig. 1b).

Life-history parameters

Offspring, juvenile and adult individuals survived to the next year with probability σ_1, σ_2, and σ_3 (Fig. 1a,b). Offspring exclusively resulted from the sexual reproduction of hermaphroditic adults with an average per capita fecundity of ϕ. Offspring individuals matured to juveniles with a maturation probability γ and stayed in the offspring stage with probability 1-γ. Survival of juveniles was reduced by intra-specific competition c following the Ricker function ($c = exp(-b * n_3)$) and thus declined with increasing adult number n_3 for overlapping generations, and with increasing juvenile number n_2 for non-overlapping generations, depending on the competition coefficient b. We also modeled a Beverton-Holt density regulation and present the results in the Supplementary Material. We focused on 4 distinct life-history strategies (*del-sem*, *del-ite*, *pre-sem*, *pre-ite*) similar to Neubert and Caswell (2000). Life histories were factorial combinations of two developmental strategies (precocious maturation - **pre**, delayed maturation - **del**) and two reproductive strategies (iteroparity - **ite**, semelparity - **sem**).

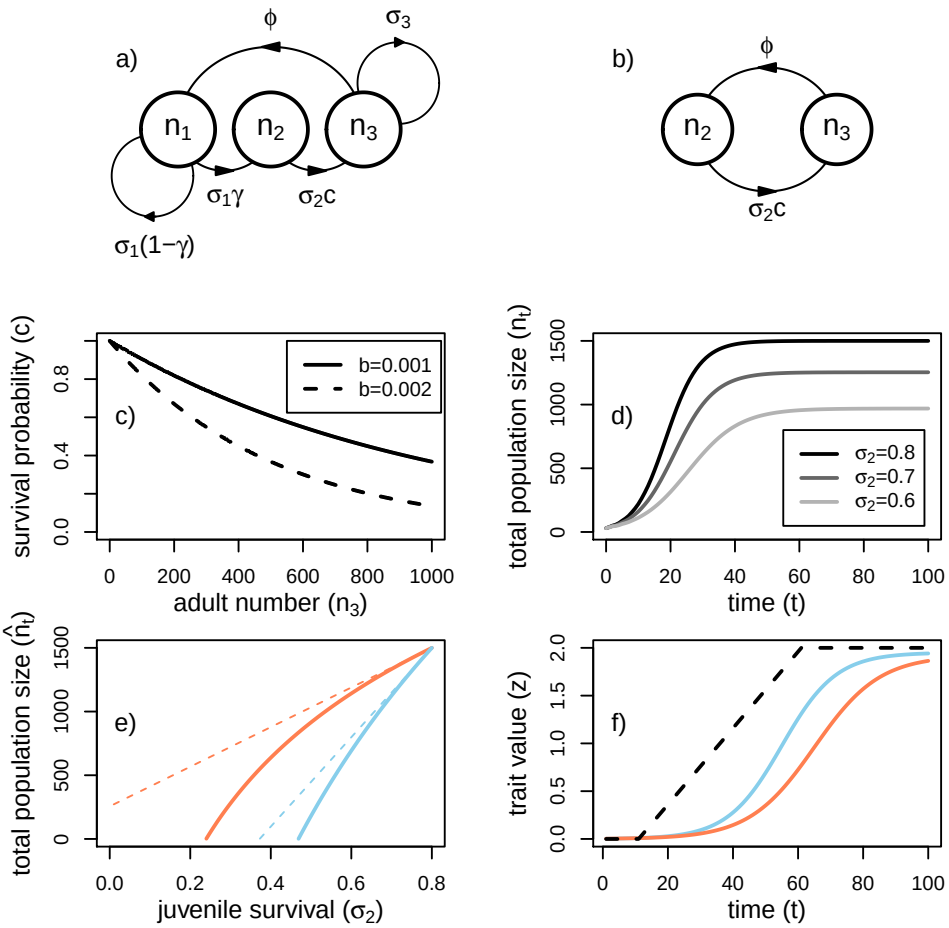

Figure 1: The life-history plot in a) illustrates the three-stage life cycle with delayed maturation and long-living adults (*del-sem*, *del-ite*, *pre-ite*), while b) shows the biennial two-stage life cycle (*pre-sem*), together with the relevant vital rates. Graph c) demonstrates the effect of negative density dependence on juvenile survival in the three-stage life cycle based on the Ricker function. Graph d) illustrates the temporal change of total population size over time following logistic growth such that an equilibrium mean population size is achieved from negative density dependence. By reducing the average juvenile survival σ_2, for instance from environmental perturbations, the population size at equilibrium $\hat{n}_t$ is reduced. We used the sensitivity of the equilibrium population size to juvenile survival ($\partial\hat{n}_t/\partial\sigma_2$) as a measure for environmental robustness. In graph e), two life histories are shown with the same equilibrium population size ($\hat{n}_t$, the two solid lines —) when environmental fluctuations are absent (at $\sigma_2 = 0.8$) but with different sensitivities to reductions in juvenile survival from interannual fluctuations. The slope of the dotted lines $(\cdots)$ in graph e) represents $\partial\hat{n}_t/\partial\sigma_2$ as how quickly $\hat{n}_t$ responds to small reductions in σ_2. Graph f) illustrates the scenario with directional environmental change and the the corresponding trait evolution of two life histories (the two solid lines —). Environmental change is realized via directional changes of the phenotypic optima (θ, dashed line $--$).

The demographic dynamics of the three-stage life cycles *del-sem*, *del-ite*, and *pre-ite* were modeled by the following matrix population model (MPM):

$$A_3 = \begin{pmatrix} \sigma_1(1-\gamma) & 0 & \phi \\ \sigma_1(\gamma) & 0 & 0 \\ 0 & \sigma_2 \cdot c & \sigma_3 \end{pmatrix}, \tag{1}$$

and the two-stage life cycle *pre-sem* was represented by the following MPM:

$$A_2 = \begin{pmatrix} 0 & \phi \\ \sigma_2 \cdot c & 0 \end{pmatrix}. \tag{2}$$

Mathematical models

the sensitivity to environmental fluctuations

We described the robustness of a life history against environmental fluctuations as the sensitivity of the total equilibrium population size $\hat{n}_t$ to juvenile survival σ_2 ($\partial\hat{n}_t/\partial\sigma_2$, Fig. 1e). Assuming that the detrimental environmental conditions exclusively reduced average σ_2, but not σ_1 or σ_3, $\partial\hat{n}_t/\partial\sigma_2$ indicated by how much the equilibrium population size (at $\lambda = 1$) was depressed by interannual environmental variability or persistent directional environmental change. Even when juveniles were perfectly adapted to the mean environmental state, the more often and the more pronounced the environment differed from optimal environmental conditions, the lower was the average juvenile survival (Chevin et al., 2017). As we

assumed that the juveniles' environmental tolerance was the same for all life histories, we expected all life histories to experience the same decline in average juvenile survival when confronted to the same degree of environmental variability. Therefore, a higher sensitivity to juvenile survival ($\partial \hat{n}_t / \partial \sigma_2$) indicated a steeper decline in total equilibrium population size from environmental perturbations, and thus a low robustness.

For the three-stage life cycle, we first derived the total population size at equilibrium $\hat{n}_t$ by solving $A_3 \cdot \hat{N} = \hat{N}$ with population vector $N = (n_1, n_2, n_3)^T$ (T meaning transposed, see Appendix A for the derivation):

$$\hat{n}_t = \frac{\phi + \phi\sigma_1\gamma - \sigma_1(1-\gamma) + 1}{b(\sigma_1(1-\gamma) - 1)} \cdot log\left(\frac{(1-\sigma_1(1-\gamma))(1-\sigma_3)}{\phi\sigma_1\gamma\sigma_2}\right). \tag{3}$$

From equation 3 we derived the partial derivative of $\hat{n}_t$ with respect to σ_2 (see Appendix A8):

$$\frac{\partial \hat{n}_t}{\partial \sigma_2} = \frac{\phi + \phi\sigma_1\gamma - \sigma_1(1-\gamma) + 1}{b\sigma_2(1-\sigma_1(1-\gamma))}. \tag{4}$$

The derivations for the two-stage life cycle are detailed in Appendix B.

An alternative measure for the robustness against environmental variability is the sensitivity of the population growth rate λ to juvenile survival ($\partial\lambda/\partial\sigma_2$), which was shown to correlate with the sensitivity of the effective population size $\hat{n}_e$, instead of the total population size n_t (Caswell et al., 2004). We present the results for $\partial \hat{n}_t / \partial \sigma_2$ together with those of $\partial\lambda/\partial\sigma_2$ (both estimated at equilibrium population density when λ=1), and discuss the differences between these two measures in Appendix C.

the rate of trait evolution

We quantified the speed of evolution for a life history as the average trait change Δz per time step t from genetic evolution (not plasticity) in response to directional selection. The speed of evolution for quantitative traits in a stage-structured population was described mathematically by Barfield et al. (2011). For a species with three life-history stages, that reached the equilibrium population size from negative density dependence, with a stable stage distribution (SSD), and with one trait under selection in juveniles (z_2), the asymptotic rate of evolution can be derived by adapting the more general solution from Barfield et al. (2011) as:

$$\Delta \bar{z} = G_2 \; v_3 \; w_2 \; \sigma_2 \; c \; \beta(z_2). \tag{5}$$

The asymptotic rate of trait change Δz thus varies with the additive genetic variance in juveniles G_2, the selection gradient on a juvenile trait $\beta(z_2)$, the fraction of individuals exposed to selection $w_2 = \frac{\hat{n}_2}{\hat{n}_t}$, the survival probability of these individuals $\sigma_2 c = \sigma_2 exp(-b\hat{n}_3)$, and their contribution to the subsequent generations v_3 (the reproductive value of adults standardized such that $v^T w = 1$) (equation 8, Barfield et al., 2011). Equation 5 assumes a population growth rate of $\lambda = 1$ at equilibrium population density, sexual (non-clonal) reproduction, weak selection, population dynamics that are faster than evolutionary dynamics, a Gaussian genotype-phenotype distribution, and a Gaussian selection function (Barfield et al., 2011; Orive et al., 2017).

The rate of evolution (Δz) then can be expressed depending on the single vital rates by deriving analytical solutions for w_2, c, and v_3 as detailed in Appendix A:

$$\Delta\bar{z} = G_2 \; \frac{(1-\sigma_3)(1-\sigma_1(1-\gamma))}{(1-\sigma_3)(1-\sigma_1(1-\gamma)) + (1-\sigma_3) + (1-\sigma_1(1-\gamma))} \; \beta(z_2) \tag{6}$$

Our definition of a life history's evolvability is similar to, but slightly deviates from, classic evolvability measures for quantitative traits. The evolvability for a single quantitative trait e is traditionally derived from the Lande equation $\Delta\bar{z} = G\beta(z)$ as the trait change per selection gradient $e = \Delta\bar{z}/\beta(z) = G$ (Hansen et al., 2019). A species' life history can be interpreted to shape Δz via both components of the Lande equation, the additive genetic variance G via the genetic storage effect, and the trait-specific selection gradient $\beta(z)$ when only a fraction of individuals is under selection. While the genetic storage effect is not accounted for in equation 6, we do account for life-history effects on the population-wide selection gradient. When further assuming $\beta(z) = 1$ for simplicity, our measure of evolvability Δz equates with e when $e = \Delta z/\beta(z) = \Delta z$. Please note that, even though we assume $\beta(z_2) = 1$, the selection gradient with a Gaussian fitness function $w(z) = exp(-(z-\theta)^2/2\omega^2)$ could be expressed as $\beta(z) = -(z-\theta)/(\omega^2 + P)$, a function of the distance between phenotype z and phenotypic optimum θ, the variance of the fitness function ω^2, and the phenotypic variance P (Via and Lande, 1985).

standardization

We standardized our generic life histories for uniform maximum population sizes ($\hat{n}_t$) in absence of environmental variation and for uniform maximum population growth rates (λ_{max}, the intrinsic population growth rate in absence of density regulation when *c=1*). With this standardization we aimed to achieve informative comparisons between life histories when keeping key demographic properties constant (see Appendix C for a detailed discussion). We standardized all life histories for a uniform maximum population growth rate λ_{max} by adjusting the fecundity ϕ using a numeric approach, and achieved the same total population size at equilibrium by adjusting the competition coefficient b using the following equation (see Appendix A for the derivation):

$$b = \frac{\phi + \phi\sigma_1\gamma - \sigma_1(1-\gamma) + 1}{n_t(\sigma_1(1-\gamma) - 1)} \cdot log\left(\frac{(1-\sigma_1(1-\gamma))(1-\sigma_3)}{\phi\sigma_1\gamma\sigma_2}\right), \tag{7}$$

such that:

$$\frac{\partial \hat{n}_t}{\partial \sigma_2} = \frac{-\hat{n}_t}{\sigma_2} \cdot log\left(\frac{(1-\sigma_1(1-\gamma))(1-\sigma_3)}{\phi\sigma_1\gamma\sigma_2}\right)^{-1}. \tag{8}$$

Using these equations we explored the effect of the vital rates σ_1, σ_3, and γ on the population size sensitivity $\partial\hat{n}_t/\partial\sigma_2$ as well as on the rate of evolution Δz (with $G = \beta(z_2) = 1$). As the sensitivity of the total population size varied with σ_2 (see equ. 8), $\partial\hat{n}_t/\partial\sigma_2$ was always quantified with $\sigma_2 = 0.8$. In addition we provide results for $\partial\lambda/\partial\sigma_2$ calculated for each combination of vital rates using the function sensitivity() from the *popbio* package (version 2.4.3, Stubben and Milligan, 2007) in R 3.4.2 (R Development Core Team, 2008).

Individual-based simulations

general

We ran individual-based simulations to test our mathematical derivations and additionally account for genetic and demographic stochasticity plus evolving additive genetic variances. Simulations were run with Nemo (Guillaume and Rougemont, 2006) extended for stage-structured populations (Cotto et al., 2017). We simulated a single panmictic population of hermaphroditic individuals. The population reached

an equilibrium population size as result of density-dependent juvenile survival. A single quantitative trait in the juvenile stage was under hard selection such that changes in juvenile fitness translated into changes of the population size. The following life cycle events occurred consecutively each year: density-dependent regulation (of juvenile survival using the Ricker function), viability selection (removal of juveniles according to their survival probability which varied with the distance between trait value and environment), sexual reproduction (independent from the environmental state or population density), and stage transitions according to the MPM.

life-history parameters

We modeled 4 generic life-history strategies as combinations of the two developmental strategies (precocious or delayed offspring maturation) and the two reproductive strategies (semelparous or iteroparous adults), in accordance with the mathematical models. We standardized all life-history strategies for the same total population size in absence of environmental fluctuations ($\hat{n}_t = 1500$ by adjusting b) and the same maximum population growth rate ($\lambda = 1.10$ or $\lambda_{max} = 1.15$, by adjusting ϕ). The single vital rates are listed in table 1.

With these simulation scenarios we tried to span a range of key life-history characteristics by accounting for differences in "pace of life" along the slow-fast continuum and for differences in the reproductive strategy (see Fig. S13, and Stearns, 1983; Gaillard et al., 1989, 2005; Salguero-Gómez, 2017).

genetic setup and selection model

We simulated evolution of a single quantitative trait (z) in the juvenile stage and used a Gaussian fitness function $w(z) = exp(-(z-\theta)^2/2\omega^2)$ to describe fitness (w) depending on the phenotype (z). Fitness was maximized with z equal to the phenotypic optimum (θ) and declined with increasing distance between z and θ depending on the variance of the fitness function (ω^2). In all of our simulations we set the variance of the fitness function to $\omega^2 = 4$ (corresponding to a stronger selection strength) or $\omega^2 = 16$ (representing a weaker selection strength). Each individual carried $l = 20$ unlinked loci, which contributed additively

Table 1: The following table lists the vital rates of the simulated life-history strategies, which are combinations of delayed (*del*, maturation probability $\gamma = 0.5$) or precocious (*pre*, $\gamma = 1.0$) offspring maturation, and semelparous (*sem*, adult survival $\sigma_3 = 0.0$) or iteroparous (*ite*, $\sigma_3 = 0.5$) adults, standardized for $\lambda_{max} = 1.10$ or $\lambda_{max} = 11.5$ via the annual fecundity ϕ. Offspring and juvenile survival were set to $\sigma_1 = \sigma_2 = 0.8$ for all life histories. The generation time (T) and the net reproductive rate (R_0) were calculated for the MPMs in absence of density regulation using the functions generation.time() and net.reproductive.rate() from the popbio package in R (Stubben and Milligan, 2007; R Development Core Team, 2008). The growth rate sensitivity ($\partial\lambda/\partial\sigma_2$) was calculated for the MPMs at $\hat{n}_t$ ($\lambda = 1$) using the function eigen.analysis() from the popbio package in R (Stubben and Milligan, 2007; R Development Core Team, 2008). The rate of evolution Δz was calculated with $G_2\beta(z_2) = 1$.

life history	λ_{max}	γ	σ_3	ϕ	b	$\partial\hat{n}_t/\partial\sigma_2[/10]$	$\partial\lambda/\partial\sigma_2$	Δz	T	R_0
del-ite	1.10	0.5	0.5	1.445	0.0012610	433.4	0.4129	0.21	4.53	1.54
del-sem	1.10	0.5	0.0	2.650	0.0016560	542.2	0.4818	0.27	3.62	1.41
pre-ite	1.10	1.0	0.5	1.134	0.0007550	503.5	0.4536	0.25	3.91	1.45
pre-sem	1.10	1.0	0.0	1.5125	0.0002111	983.6	0.6250	0.50	2.00	1.21
del-ite	1.15	0.5	0.5	1.750	0.0021100	301.1	0.5000	0.21	4.47	1.87
del-sem	1.15	0.5	0.0	3.100	0.0027600	372.9	0.5636	0.27	3.60	1.65
pre-ite	1.15	1.0	0.5	1.343	0.0012340	346.2	0.5372	0.25	3.88	1.72
pre-sem	1.15	1.0	0.0	1.6530	0.0002990	671.0	0.6250	0.50	2.00	1.32

to single quantitative trait z. The trait value of an individual was calculated as the sum of allelic effects (a) across all loci l and both homologous copies j (e.g., z=$\sum_{l=1}^{20}\sum_{j=1}^{2} a_{lj}$). We used a continuum-of-allele model where mutational effects were picked from a Gaussian distribution centered at zero with a mutational variance of $\alpha^2 = 0.1$. The mutation rate was set to $\mu = 0.0001$ such that the mutational phenotypic variance was $V_M = 2l\mu\alpha^2 = 0.001$. We excluded random environmental effects on phenotype expression (e.g., developmental noise) such that the phenotype z was the sole product of the additive genetic effects for simplicity.

environmental scenarios

We simulated environmental variation between years together with gradual changes of the average condition by perturbing the phenotypic optimum θ (e.g., see Chevin et al., 2017). Each year, the position of the phenotypic optimum for the entire population was picked from a Gaussian distribution $\theta \sim \mathcal{N}(\bar{\theta},\epsilon)$ with the average environment $\bar{\theta}$ and variance ϵ. We thus simulated environmental fluctuations between years that were independently and identically distributed (e.g., Caswell, 2001).

To asses the population size sensitivity of life-history strategies to interannual environmental stochasticity, we ran burn-in simulations over 50'000 years to reach mutation-selection balance and allow G_2 to reach equilibrium levels in accordance with the respective life history. Burn-in simulations were run with a constant average environment of $\bar{\theta} = 10$ for six different degrees of environmental fluctuations ($\epsilon = 0.0, 0.2, 0.5, 1.0, 1.5, 2.0$) and populations were stored after 50'000 years. We then loaded the stored populations, ran additional simulations under the same conditions for 500 years, and recorded population characteristic (e.g., population size $\hat{n}_t$) every 10 years. A life history's population size sensitivity to environmental variability was assessed as the steepness of declining average population sizes ($\hat{n}_t = \frac{1}{51}\sum_{t=1}^{500} n_t$) with increasing degrees of interannual environmental fluctuations.

To asses the speed of trait evolution, we loaded the post-burn-in populations and initiated directional environmental change of the average environmental condition ($\bar{\theta}$), while still simulating interannual variation on top of the changing mean. The average phenotypic optimum at t=100 then started to change with a rate of $\Delta\bar{\theta}$=+0.01, either for 200 years or for 800 years. We quantified the speed of evolution as the time to evolve 90% of the novel phenotypic optimum ($\bar{\theta}$=12, or $\bar{\theta}$=18). We did not used the maximum rate of phenotypic change per time step because all life histories either went extinct or adopted trait changes as fast as the rate of environmental change ($\Delta z = \Delta\bar{\theta}$).

We thus ran simulations for 196 parameter combinations with 4 different life-history strategies, 2 maximum growth rates (λ_{max}), 2 selection strength levels (ω^2), 6 different degrees of interannual environmental fluctuations (ϵ), and 2 different lengths of environmental change (200 and 800 years). For each parameter combination we ran 100 replicates.

Results

Mathematical model

general findings

We found a tradeoff between life-history effects on the rate of evolution and their robustness against environmental perturbations in the mathematical models, at least when comparing life histories with the same maximum growth rate to each other. We found a positive, linear relationship between the rate of evolution (Δz) and the sensitivity of the population size to juvenile survival ($\partial n_t/\partial\sigma_2$ and $\partial\lambda/\partial\sigma_2$) across both kinds of models, the three-stage model as well as the two-stage model (Fig. 2). Changes in vital rates that enhanced the rate of evolution also increased the sensitivity to environmental perturbations, and vice versa.

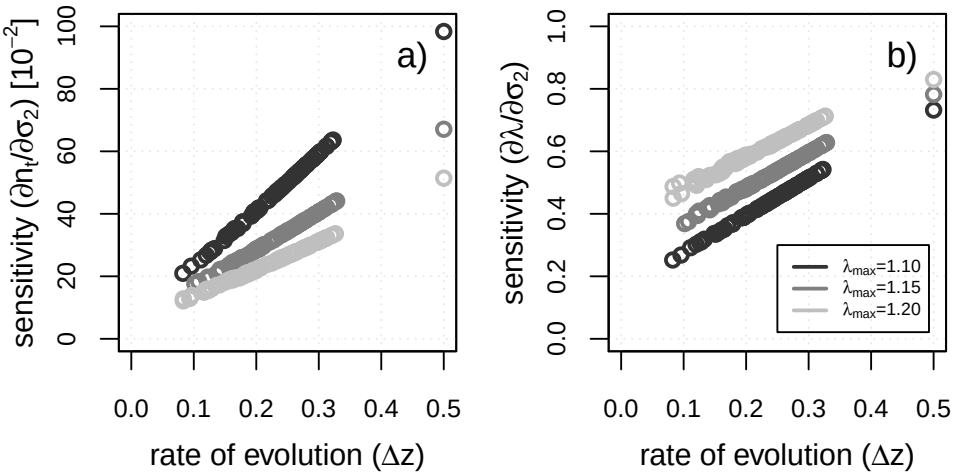

Figure 2: A life history's tradeoff between evolvability (Δz) and robustness ($\partial\hat{n}_t/\partial\sigma_2$ in a, and $\partial\lambda/\partial\sigma_2$ in b). Each circle illustrates a random combination of vital rates (with $0.2 \leq \sigma_1 \leq 1.0$, $\sigma_2 = 0.8$, $0.0 \leq \sigma_3 \leq 0.9$, $0.2 \leq \gamma \leq 1.0$). The fecundity (ϕ) and the strength of competition (b) were re-calculated for each vital rate combination to standardize the maximum population growth rate ($\lambda_{max} = 1.10 - black, \lambda_{max} = 1.15 - darkgray, \lambda_{max} = 1.20 - lightgray$) and the total population size at stable conditions (n_t=1'500). We then calculated the rate of evolution (Δz, with $G_2\beta(z_2) = 1$), the population size sensitivity ($\partial\hat{n}_t/\partial\sigma_2$), and the growth rate sensitivity ($\partial\lambda/\partial\sigma_2$) for each life-history variant. The three single points on the right of the plots were derived for the 2-stage life cycle (with $\sigma_2 = 0.8$), while the rest of the points illustrate parameter combinations for 3-stage life cycles.

the effect of single vital rates

Our models indicate that a higher degree of iteroparity (high adult survival σ_3; Fig. 3a,d,g) and a larger extent of dormancy (low maturation rate γ; Fig. 3c,f) reduced the population size sensitivity to environmental fluctuations, but came at the expense of a lower rate of directional trait evolution. In contrast, precocious maturation and semelparous adults allowed for fast evolution but elevated the robustness to environmental variability. The maximum rate of population growth (λ_{max}) shaped the population size sensitivity to environmental fluctuations, even though it had no effect on the rate of evolution. Higher λ_{max} reduced $\partial n_t/\partial\sigma_2$ and thus helped to maintain higher population densities with short-term environmental perturbations (Fig. 2), equation 8). Instead, the maximum growth rate had no consequences for the rate of evolution, at least when Δz was measured in our models for populations at carrying capacity ($\hat{n}_t$) with a growth rate at unity ($\lambda = 1$) (see also equation 6).

growth rate sensitivity $\partial\lambda/\partial\sigma_2$

The alternative measure for a life history's robustness against environmental variability $\partial\lambda/\partial\sigma_2$ gave the same qualitative model outcomes as $\partial\hat{n}_t/\partial\sigma_2$, at least for a given maximal growth rate (Fig. 2). However, $\partial\lambda/\partial\sigma_2$ responded differently to changes in λ_{max}. While a higher maximum growth rate reduced the population size sensitivity, it increased the growth rate sensitivity. In other words, vital rate changes that increased the populations' maximal growth rate and helped to maintain higher population sizes in the face of interannual environmental fluctuations caused stronger declines in the effective population size (Fig. 3h, Fig. 3g-i).

density regulation

The tradeoff between the rate of evolution (Δz) and the robustness against environmental variation ($\partial\hat{n}_t/\partial\sigma_2$, and $\partial\lambda/\partial\sigma_2$) was also found when using the Beverton-Holt function instead of the Ricker function for density regulation (Fig. S5). The levels of Δz and $\partial\hat{n}_t/\partial\sigma_2$ were identical for both functions, while the sensitivity levels $\partial\hat{n}_t/\partial\sigma_2$ were higher with a Beverton-Holt than with a Ricker function (Fig. S6). However, there was still a positive linear relationship between both functions such that the tradeoff

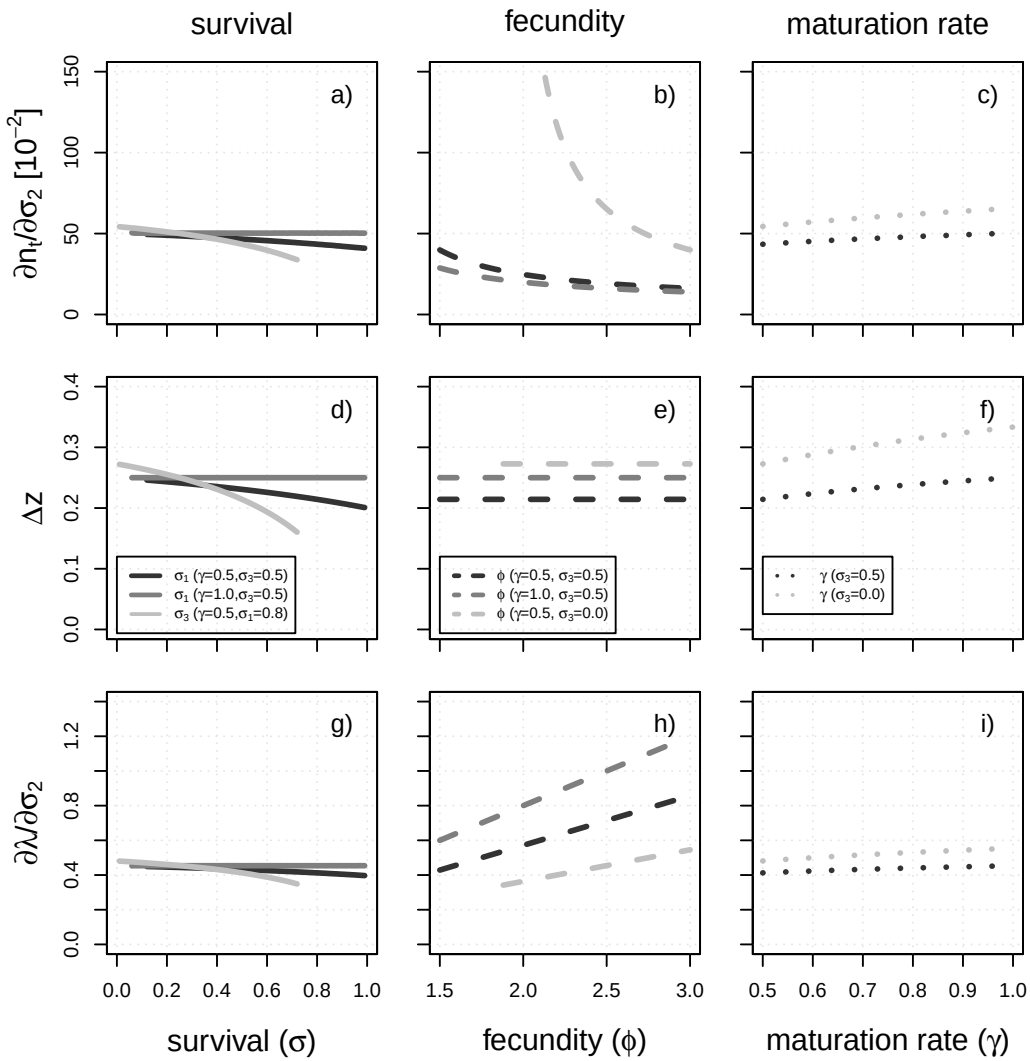

Figure 3: The graphs illustrate the analytical results for the sensitivity of the total population size to juvenile survival ($\partial\hat{n}_t/\partial\sigma_2 10^{-2}$, a-c), the rate of evolution (Δz, d-f), and the sensitivity of the population growth rate ($\partial\lambda/\partial\sigma_2$, g-i) for three-stage life cycle depending on survival rate (σ_1, σ_3), fecundity (ϕ), and maturation probability (γ). The sensitivity measures ($\partial\lambda/\partial\sigma_2$, $\partial\hat{n}_t/\partial\sigma_2$) were estimated at equilibrium population size in absence of interannual environmental variation at $\sigma_2 = 0.8$. The maximum growth rate has been standardized for $\lambda_{max} = 1.10$ by fecundity adjustments, except for the case with varying fecundity (b,e,h). Each parameter combination has been standardized for the same equilibrium population size in absence of interannual environmental fluctuations ($\hat{n}_t$=1500) via adjustments of the strength of competition (b). If not specified otherwise, the following parameter values have been used : $\sigma_1 = 0.8$, $\sigma_3 = 0.5$, $\gamma = 0.5$, $G = 1$, and $\beta(z_2) = 1$.

was maintained (Fig. S5).

Individual-based simulations

general findings

We could confirm the tradeoff between evolvability and robustness also in our individual-based simulations as the genetic storage effect was not strong enough to overcome the tradeoff. Life-history strategies with high robustness had the slowest rates of evolution, and vice versa. The average population size maintained at constant average conditions during burn-in declined with increasing environmental fluctuations for all life cycles below $\hat{n}_t = 1'500$, while life-history strategies differed from each other in the extent of $\hat{n}_t$ reductions (Fig. 4b, Fig. 5a). The onset of gradual environmental change further reduced juvenile survival and evoked a decline in juvenile number and total population size (Fig. 4b,d), before trait evolution allowed to adapt to the changing conditions (Fig. 4a) and recover in a later phase of environmental change (Fig. 4d). Evolutionary rescue resulted in a u-shaped curve in total population size n_t, with a population size recovery already during environmental change or only after environmental change has stopped (Fig. 4b).

population size sensitivity to environmental variability

The sensitivity of the total population size to juvenile survival as predicted from our analytical models (Tab. 1) matched with our simulations results (Fig. 5a). The biennial, two-stage life cycle (*pre-sem*) experienced the greatest n_t declines from interannual environmental fluctuation and thus had the highest sensitivity, followed by the *pre-ite*, *del-sem*, and the *del-ite* life history. This rank order of life-history strategies was found for both maximum population growth rates, with life histories standardized for $\lambda_{max} = 1.15$ exhibiting higher robustness against environmental variability than those with $\lambda_{max} = 1.10$ (Fig. 5a). This rank order was further maintained across both strengths of selection, even though the decline in $\hat{n}_t$ with ϵ was much lower for $\omega^2 = 16$ than for $\omega^2 = 4$ (Fig. S11).

The fluctuations in the total population size ($\hat{n}_t$) over time increased with interannual environmental

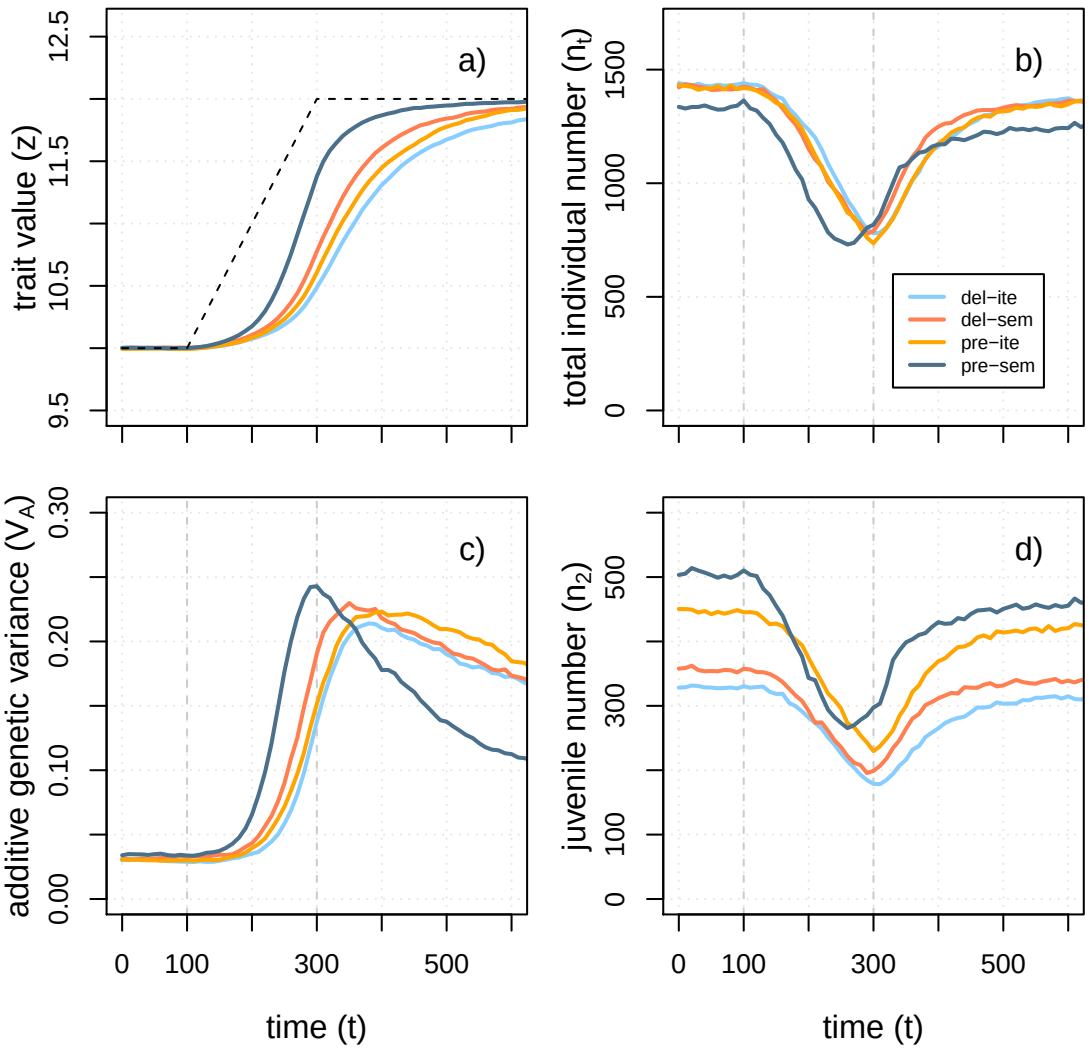

Figure 4: The graphs show the results of individual-based simulations for the mean trait value z (a), the total population size n_t (b), the additive genetic variance G_2 (c), and the juvenile number n_2 (d) for the four life histories (*del-sem*, *del-ite*, *pre-ite*, *pre-sem*) over 600 years. Environmental change started at t=100 and was realized by a gradual shift in the phenotypic optimum (−− black dashed lines) from $\theta = 10$ to $\theta = 12$ by t=300 (a). The between-year environmental fluctuations were set to $\epsilon = 0.2$ and life histories were standardized for $\lambda_{max} = 1.15$. Average population sizes (n_t) were standardized to $n_t = 1500$ in absence of interannual environmental fluctuations, and were depressed as result of between-year fluctuations and directional environmental change as result of a fitness reduction in juveniles (a). All values of the total population size and trait values represent the arithmetic means over all of the 100 replicates that did not went extinct.

fluctuations (ϵ) for all life cycles, while the extent strongly differed between life-history strategies (Fig. 5b). With increasing ϵ, the breadth of the 90% quantile of total population sizes increased strongest for the biennial life cycle (*pre-sem*) and slowest for the iteroparous life cycle with delayed maturation (*del-ite*). While this rank order was qualitatively identical with the order of life histories' sensitivity to environmental variation ($\partial\hat{n}_t/\partial\sigma_2$), life histories standardized for $\lambda_{max} = 1.15$ did not exhibit considerably lower stochasticity than those standardized for $\lambda_{max} = 1.10$ (compare the dashed lines between Fig. 5 a and b). The stochasticity in $\hat{n}_t$ resulting from interannual environmental fluctuations was strongly attenuated by a weaker strength of selection (Fig. S11).

rate of directional trait evolution

The speed of evolution differed among life histories in accordance with the analytical predictions (Table 1). The biennial life cycle (*pre-sem*) could respond most quickly to directional environmental change via trait evolution, while the *del-ite* life history evolved the slowest (Fig. 5c). A weaker strength of selection ($\omega^2 = 16$) reduced the speed of trait evolution for all life histories, but did not change the life histories' rank order in this regard (Fig. S11). However, differences in evolvability were only found on absolute time scales, as all life histories took a similar (though not exactly identical) number of generations to reach the phenotypic threshold (Fig. S10c). Even though the differences were small, life histories standardized for $\lambda_{max} = 1.15$ evolved faster than life histories with $\lambda_{max} = 1.10$ (Fig. 5c), which was a deviation from the analytical predictions.

While the level of standing genetic variation G_2 during burn-in increased slightly with environmental variance for all life histories, no distinct differences in G_2 were observed between life-history strategies (Fig. 5d). However, we did observe differences between life histories in the temporal changes of G_2 over the course of directional selection (Fig. 4c, Fig. S8). The rise and fall in additive genetic variance was fastest for the biennial life cycle *pre-sem* and slowest for the life cycle with delayed maturation and iteroparous adults *del-ite* (Fig. 4). A lower strength of selection ($\omega^2 = 16$) led to higher levels of G_2 for all four life histories (Fig. S11).

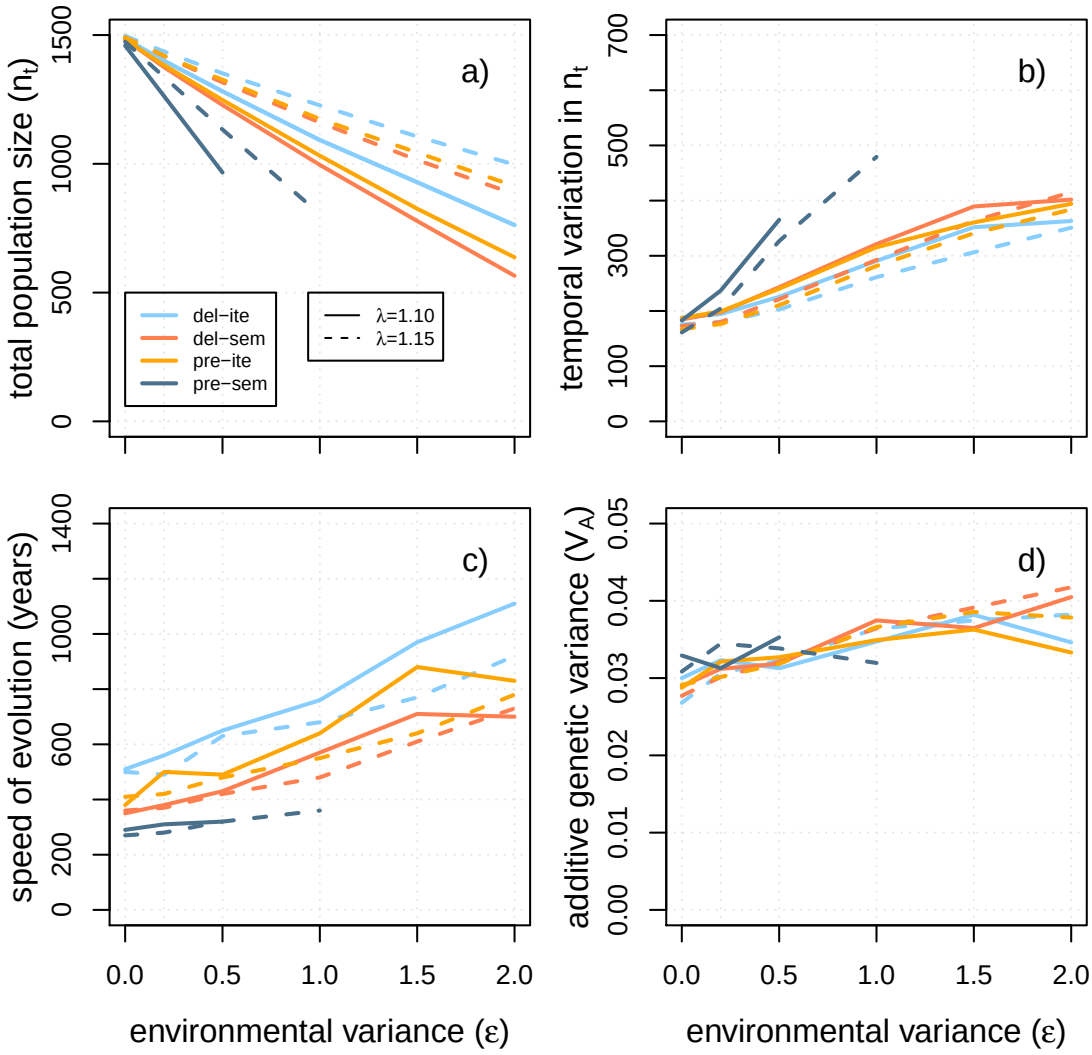

Figure 5: The graphs illustrate the total population size n_t (a), the variability in n_t over time (90 % quantile of n_t over 500 years, b), the speed of evolution (the average number of years to reach the trait value $z = 11.8$, c), and the additive genetic variance (G_2, d) are shown depending on the interannual environmental variability (ϵ). The simulation results are shown for four life histories (*del-sem*, *del-ite*, *pre-ite*, *pre-sem*) that have been standardized for two maximal population growth rates ($\lambda_{max} = 1.10$, $\lambda_{max} = 1.15$) with environmental change lasting for 200 years.

extinction risk

Life histories diverged from each other in their extinction risks, both in the extinction dynamics over time as well as in the total number of extinct replicates at the end of the simulations (Fig. 6). Population extinctions were delayed with regard to the onset of directional environmental change and continued to occur even when the environmental change had already been stopped (Fig. 6a,c). Life-history strategies

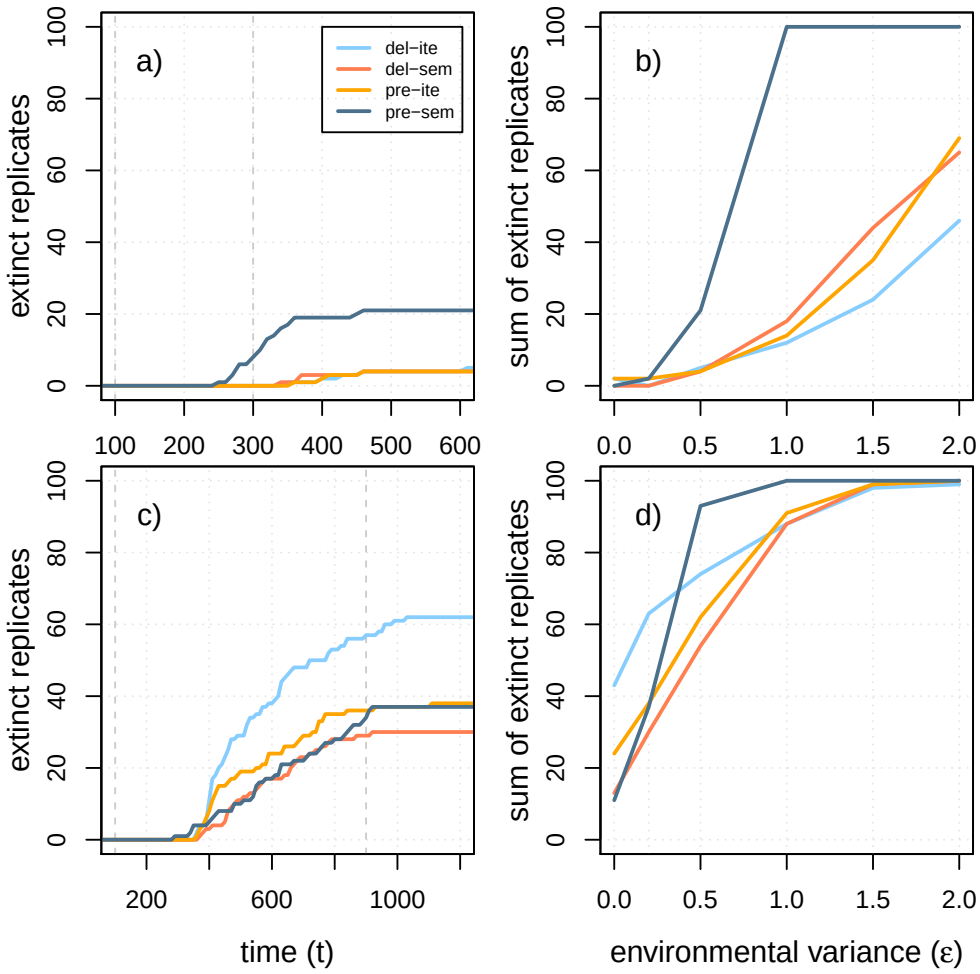

Figure 6: These graphs show the number of extinct replicates over time t (a,c) and the total number of extinct replicates depending on environmental variability ϵ (b,d) for each of the four life histories. Extinction dynamics are shown for two different scenarios with environmental change either lasting for 200 years (a,b) or for 800 years (c,d). The gray dashed lines indicate the start of environmental change ($t = 100$) and its end ($t = 300$ for a,b; $t = 900$ for c,d). In both scenarios, the rate of environmental change per year was set to $\Delta\bar{\theta} = 0.01$ and all life histories were standardized for a maximum growth rate of $\lambda = 1.10$. The temporal dynamics are shown for an environmental variability of $\epsilon = 0.5$ (a) and $\epsilon = 0.2$ (c).

more sensitive to environmental perturbations (e.g., *pre-sem*) experienced extinctions earlier than less sensitive life histories (e.g., *del-ite*). Faster extinction of more sensitive life-history strategies derived from lower average population densities in face of environmental variability after burn-in, more pronounced population size fluctuations over time, and a faster population size decline during the initial phase of environmental change (Fig. 4b,d). However, a weaker selection strength ($\omega^2 = 16$) helped to avoid

extinctions altogether (Fig. S12).

The proportion of extinct simulation replicates increased with the degree of environmental fluctuations for all life histories and was higher for environmental change lasting for 800 years than for environmental change over 200 years (Fig. 6b,d). In all our simulations, the extinction probability of a life history was higher with a maximum growth rate of $\lambda_{max} = 1.10$ than with $\lambda_{max} = 1.15$ (Fig. S9). The life histories' rank order of extinction risk varied with the duration of environmental change and the extent of interannual environmental variability. With environmental change for 200 years, the biennial life cycle (*pre-sem*) experienced the highest number of extinct replicates for almost all levels of environmental variability, especially compared to the *del-ite* life history (Fig. 6b). This pattern was reversed with long-lasting environmental change over 800 years such that *pre-sem* experienced lower extinction levels than "slower" life histories (Fig. 6d). However, this benefit of the biennial life cycle only hold at weak interannual environmental variation but was mostly reversed again when long directional environmental change was combined with high environmental variance (Fig. 6d).

Discussion

General

Life-history strategies can impact a species' persistence in a dynamic environment, especially by helping to cope with short-term interannual fluctuations and by shaping the evolutionary response to long-term gradual changes (Lande, 1982; Hairston and De Stasio Jr., 1988; Barfield et al., 2011). In this theoretical study we tested for a tradeoff between a life history's robustness against environmental variability and its effect on the rate of trait evolution. We derived mathematical models and ran individual-based simulations for a single population reaching a carrying capacity under negative density dependence. Individuals in the offspring and adult stages were shielded from detrimental environmental conditions, while only juveniles were under selection. We could confirm the hypothesized tradeoff between a life history's robustness and evolvability with both approaches, mathematical models and simulations, at least when comparing life histories with the same maximum growth rate to each other. Dormancy in offspring and iteroparity in

adults led to higher robustness against environmental fluctuations but slowed down the speed of evolution. Immediate maturation and semelparity reduced robustness but increased evolvability. The genetic storage effect was not strong enough to overcome this tradeoff, at least for the explored parameter range. The simulations further demonstrated that robustness and evolvability fed back on the extinction risks in a temporally varying environment. While "evolvable" life-history strategies could cope best with long-lasting directional environmental change, they experienced the highest extinction risk from interannual environmental variation and during the initial phase of environmental changes.

A tradeoff between robustness and evolvability

A higher robustness against between-year environmental fluctuations was achieved by three life-history characteristics. Offspring dormancy and higher survival in adults helped to tolerate a variable environment by shielding a higher proportion of individuals from detrimental environmental conditions and spreading the risk of failed survival across years (e.g., see also Orzack and Tuljapurkar, 1989; Tuljapurkar, 1990; Koons et al., 2008; Zeineddine and Jansen, 2009). In our simulations, offspring dormancy and long-living iteroparous adults allowed to maintain high population sizes in face of fluctuations, reduced stochasticity in population densities, and thereby helped to cope with interannual environmental variation as well as with maladaptedness during the initial phase of environmental change. In addition, a larger growth rate improved the robustness to environmental variability (e.g., see Hallett et al., 2018) by helping to recover quickly from extreme events, and reducing the importance of environmental variation for population densities relative to the effect of intra-specific competition.

Opposed to the means of promoting robustness, evolvability of life-history strategies increased with lower dormancy in offspring and smaller adult survival, which is in line with two rules of thumb. First, the rate of trait evolution could be elevated by exposing more individuals to selection and improving their contribution to the next generation (Hairston and De Stasio Jr., 1988; Barfield et al., 2011). The same result has been described before by Kuparinen et al. (2010) who simulated the evolution of a quantitative trait in Scots pine and Silver birch. A higher mortality in adult trees from disturbances (e.g., forest fires or forest management) or from age-dependent mortality (senescence) was one major way of speeding

up evolution in their simulations. As a second rule of thumb, evolution could be accelerated by shorter generation times and a faster turn-over of the gene pool (Barfield et al., 2011; Orive et al., 2017). Osmond et al. (2017) described this mechanism in predator-prey systems when predation reduced the generation time of the prey species and thus helped the prey to better adapt to novel environmental conditions. We thus could confirm the initial hypothesis as those life-history changes favoring evolvability simultaneously reduced robustness to interannual environmental variability, and vice versa.

Life-history effects on the additive genetic variance

We hypothesized that the tradeoff between robustness and evolvability for life histories could be overcome via the genetic storage effect, which was not confirmed by our simulations. Even though the storage effect has indeed been shown to speed up evolution for very large environmental fluctuations (Yamamichi et al., 2019), we could not impose such high levels of ϵ without driving populations to extinction. We installed hard selection to quantify the decline in individual numbers with increasing environmental variability, while Yamamichi et al. (2019) simulated a yearly offspring production that was insensitive to ϵ. As a consequence, our simulations resulted in similar levels of standing genetic variation across life histories, even though a stronger manifestation of the genetic storage effect could be achieved for (very) different scenarios (Yamamichi et al., 2019).

While we could not confirm a pronounced effect of the genetic storage effect, life-history strategies differed distinctly from each other in the evolution of G_2 in the course of environmental change. The additive genetic variance within populations G_2 increased during directional selection in all our simulations. The rise in G_2 with environmental changes resulted from increasing allele frequencies of rare variants (Bürger, 1999; Kopp and Matuszewski, 2014), and happened most rapidly for the biennial life cycle and slowest for the life history with offspring dormancy and iteroparity. When a higher proportion of juveniles under selection allowed for faster allele frequency changes over time, the additive genetic variance levels raised more quickly, and thus boosted evolution for these life-history strategies. Life histories thus shaped the rate of evolution via G_2 differently from our initial expectations, in fact in the opposite direction, such that the tradeoff was not mitigated but enforced.

How the tradeoff could be overcome

Some life-history strategies could be more robust and at the same time more evolvable than other life histories when deviating from a strict standardization, and exhibiting a higher maximum growth rate. In our mathematical models and simulations, a higher growth rate λ_{max} increased the robustness against environmental fluctuations and thus helped to better cope with short-term environmental variability, in line with previous theory (Lande, 1993; Bürger and Lynch, 1995; Bürger, 1999; Hallett et al., 2018). Interestingly, a higher growth rate also caused faster trait evolution in our simulations, even though it had no effect on Δz in our mathematical models. In the simulations, a higher λ_{max}, when realized by larger fecundity, was associated with more frequent mutation and recombination events. This effect of life-history parameters on the mutational input was a process not accounted for in the mathematical derivation, but could be of potential importance in natural systems.

As a consequence, a higher growth rate reduced the extinction risk from both short- and long-term environmental changes for all life histories. This outcome is in line with similar theoretical studies indicating that a higher growth rate could make evolutionary rescue more likely (Lynch et al., 1991; Lynch and Lande, 1993). Here, the potential to commit evolutionary rescue was not only a matter of phenotypic trait changes via evolution, but integrated ecological properties as well, including the intrinsic growth rate, generation time, total population sizes, and phenotypic plasticity (Lynch et al., 1991; Lynch and Lande, 1993; Bürger and Lynch, 1995; Gomulkiewicz and Holt, 1995; Chevin et al., 2010). Given that a life history's robustness and evolvability could be improved simultaneously via λ_{max}, the described tradeoff between these properties should only be detectable in empirical tests when applying "fair" comparisons between (highly) standardized life histories.

Extinction risks in a temporally varying environment

Naively one could expect that those life histories allowing for the fastest rate of trait evolution would cope best with directional environmental change, which was not necessarily found in this study. When high evolvability of a life history came at the expense of a low robustness, evolvable life histories experienced severe population size declines in the early phase of environmental change before evolutionary rescue

allowed populations to recover. Instead, robust life-history strategies with low evolvability allowed best to survive the beginning of directional environmental changes as they could cope best with reduced juvenile survival from maladaptedness. The ability for evolutionary rescue gained in importance only in a later phase of environmental change when directional trait changes were necessary for population recovery. Ecological factors thus might play a key role in the early phase of environmental change, while the importance of evolutionary processes dominates later on.

Implications

Even though we could confirm the tradeoff between robustness and evolvability for life-history strategies when applying strict standardization, life-history strategies in natural systems are rarely standardized. In fact, systematic differences in more than one character are the rule rather than the exception. Species with low generations times often exhibit systematically higher population sizes ($\hat{n}_t$ and n_e), greater intrinsic growth rates, larger dispersal abilities, but lower competitive abilities than species with long generation times (Petit and Hampe, 2006; Buoro and Carlson, 2014; Beckman et al., 2018). It thus remains to be further investigated whether life-history strategies could overcome the evolvability robustness tradeoff also by other means than λ_{max}, or whether some life-history strategies are indeed more prone to certain environmental dynamics than others.

Acknowledgements

We thank Thomas F. Hansen, Luis-Miguel Chevin, and Richard Gomulkiewicz for insightful discussions and comments on the manuscript.

Appendix

Appendix A: 3-stage model

Equilibrium population size

The populations' demographic dynamics were modeled via the population vector

$$N = \begin{pmatrix} n_1 \\ n_2 \\ n_3 \end{pmatrix} \tag{A1}$$

and the matrix population model

$$A = \begin{bmatrix} \sigma_1(1-\gamma) & 0 & \phi \\ \sigma_1(\gamma) & 0 & 0 \\ 0 & \sigma_2 \cdot exp(-bn_3) & \sigma_3 \end{bmatrix} \tag{A2}$$

such that $N(t+1) = AN(t)$. By solving for the stage densities at equilibrium when $\hat{N} = A\hat{N}$,with $\hat{N} = (\hat{n}_1, \hat{n}_2, \hat{n}_3)^T$, the individual numbers within the offspring, juvenile, and adult stage at equilibrium could be derived as

$$\hat{n}_1 = \frac{\phi}{b(\sigma_1(1-\gamma)-1)} \cdot log\left(\frac{(1+\sigma_1\gamma-\sigma_1)(1-\sigma_3)}{\phi\sigma_1\gamma\sigma_2}\right), \tag{A3}$$

$$\hat{n}_2 = \frac{\phi\sigma_1\gamma}{b(\sigma_1(1-\gamma)-1)} \cdot log\left(\frac{(1+\sigma_1\gamma-\sigma_1)(1-\sigma_3)}{\phi\sigma_1\gamma\sigma_2}\right), \tag{A4}$$

$$\hat{n}_3 = \frac{1}{-b} \cdot log\left(\frac{(1+\sigma_1\gamma-\sigma_1)(1-\sigma_3)}{\phi\sigma_1\gamma\sigma_2}\right). \tag{A5}$$

The total population size at equilibrium was computed from $\hat{n}_t = \hat{n}_1 + \hat{n}_2 + \hat{n}_3$ as

$$\hat{n}_t = \frac{\phi+\sigma_1\gamma(\phi+1)-\sigma_1+1}{b(\sigma_1(1-\gamma)-1)} \cdot log\left(\frac{(1+\sigma_1\gamma-\sigma_1)(1-\sigma_3)}{\phi\sigma_1\gamma\sigma_2}\right). \tag{A6}$$

Sensitivity of total population size to juvenile survival

The partial derivative of the total population size at equilibrium ($\hat{n}_t$) to juvenile survival (σ_2) was calculated as

$$\frac{\partial\hat{n}_t}{\partial\sigma_2} = \frac{\phi+\sigma_1\gamma(\phi+1)-\sigma_1+1}{b(\sigma_1(1-\gamma)-1)} \cdot \frac{\phi\sigma_1\gamma\sigma_2}{(1+\sigma_1\gamma-\sigma_1)(1-\sigma_3)} \cdot \left(\frac{-1\phi\sigma_1\gamma(1+\sigma_1\gamma-\sigma_1)(1-\sigma_3)}{(\phi\sigma_1\gamma\sigma_2)^2}\right), \tag{A7}$$

which could be simplified to

$$\frac{\partial\hat{n}_t}{\partial\sigma_2} = \frac{\sigma_1(1-\gamma)-1-\phi(1+\sigma_1\gamma)}{b\sigma_2(\sigma_1(1-\gamma)-1)}. \tag{A8}$$

To standardize a life history for a specific total equilibrium population size ($\hat{n}_t$) the strenght of intraspecific competition was adjusted as follows

$$b = \frac{\phi+\sigma_1\gamma(\phi+1)-\sigma_1+1}{\hat{n}_t(\sigma_1(1-\gamma)-1)} \cdot log\left(\frac{(1+\sigma_1\gamma-\sigma_1)(1-\sigma_3)}{\phi\sigma_1\gamma\sigma_2}\right). \tag{A9}$$

By inserting equation A9 in equation A8, the population size sensitivity can be expressed depending on the equilibrium population size as

$$\frac{\partial\hat{n}_t}{\partial\sigma_2} = \frac{\sigma_1(1-\gamma)-1-\phi(1+\sigma_1\gamma)}{\sigma_2(\sigma_1(1-\gamma)-1)} \cdot \frac{\hat{n}_t(\sigma_1(1-\gamma)-1)}{\phi+\sigma_1\gamma(\phi+1)-\sigma_1+1} \cdot log\left(\frac{(1+\sigma_1\gamma-\sigma_1)(1-\sigma_3)}{\phi\sigma_1\gamma\sigma_2}\right)^{-1}, \tag{A10}$$

such that the following partial derivative is obtained

$$\frac{\partial \hat{n}_t}{\partial \sigma_2} = \frac{-\hat{n}_t}{\sigma_2} \cdot log\left(\frac{(1+\sigma_1\gamma-\sigma_1)(1-\sigma_3)}{\phi\sigma_1\gamma\sigma_2}\right)^{-1}. \tag{A11}$$

Rate of evolution at equilibrium population size

We adapted equation 8 from Barfield et al. (2011) for our three-stage life cycle to describe the rate of evolution depending on the juvenile proportion (w_2), juvenile survival (σ_2), competition survival (c), the reproductive value of adults (v_3), the additive genetic variance in juveniles (G_2), and the selection gradient on a juvenile trait ($\beta(z_2)$) as

$$\Delta\bar{z} = G_2\ v_3\ w_2\ \sigma_2\ c\ \beta(z_2). \tag{A12}$$

The juvenile proportion (w_2) could be derived from equation A4 and A6 as

$$w_2 = \frac{\hat{n}_2}{\hat{n}_t} = \frac{\phi\sigma_1\gamma}{\phi+\sigma_1\gamma(\phi+1)-\sigma_1+1}. \tag{A13}$$

The probability of surviving intra-specific competition (c) was derived by combining the Ricker function $c = exp(-bn_3)$ and equation A5 as

$$c = \frac{(1-\sigma_3)(1+\sigma_1\gamma-\sigma_1)}{\phi\sigma_1\gamma\sigma_2}. \tag{A14}$$

The reproductive value of adults (v_3) could be derived from the left eigenvector (v) of the matrix population model (A) when solving $vA = \lambda v$ (Caswell, 2001, equation 4.81). For a population at equilibrium population size ($\lambda = 1$) the reproductive value of adults can be derived as

$$v_3 = \frac{\phi}{(1-\sigma_3)}, \tag{A15}$$

and normalized to

$$v_3 = \frac{\phi + \sigma_1\gamma(\phi + 1) - \sigma_1 + 1}{(1 - \sigma_3)(1 - \sigma_1(1 - \gamma)) + (1 - \sigma_3) + (1 - \sigma_1(1 - \gamma))} \tag{A16}$$

such that $v * w = 1$ (as in Barfield et al., 2011). The rate of evolution depending on the single vital rates then could be expressed as

$$\Delta\bar{z} = G_2 \; \frac{(1 - \sigma_3)(1 - \sigma_1(1 - \gamma))}{(1 - \sigma_3)(1 - \sigma_1(1 - \gamma)) + (1 - \sigma_3) + (1 - \sigma_1(1 - \gamma))} \; \beta(z_2). \tag{A17}$$

Appendix B: 2-stage model

Equilibrium population size

The demographic dynamics for a 2-stage life history with non-overlapping generations were modeled by the population vector

$$N = \begin{pmatrix} n_2 \\ n_3 \end{pmatrix} \tag{B1}$$

and the matrix population model

$$A = \begin{bmatrix} 0 & \phi \\ \sigma_2 exp(-bn_2) & 0 \end{bmatrix} \tag{B2}$$

such that $N(t+1) = AN$. By solving for the individual numbers within stages at equilibrium when $\hat{N} = A\hat{N}$ and $\hat{N} = (\hat{n}_2, \hat{n}_3)^T$ the juvenile and adult numbers at equilibrium were derived as

$$\hat{n}_2 = \frac{-\phi}{b\phi} \cdot log\left(\frac{1}{\phi\sigma_2}\right). \tag{B3}$$

$$\hat{n}_3 = \frac{-1}{b\phi} \cdot log\left(\frac{1}{\phi\sigma_2}\right). \tag{B4}$$

(with natural logarithm log()). The total population size at equilibrium was computed from $\hat{n}_t = \hat{n}_2 + \hat{n}_3$ as

$$\hat{n}_t = \frac{-1-\phi}{b\phi} \cdot log\left(\frac{1}{\phi\sigma_2}\right). \tag{B5}$$

Sensitivity of total population size to juvenile survival

The partial derivative of the total population size at equilibrium $\hat{n}_t$ to juvenile survival σ_2 was derived as

$$\frac{\partial \hat{n}_t}{\partial \sigma_2} = \frac{(-\phi - 1)}{b\phi} \cdot \frac{\sigma_2 \phi}{1} \cdot \frac{-\phi}{\phi^2 \sigma_2^2}, \tag{B6}$$

which could be simplified to

$$\frac{\partial \hat{n}_t}{\partial \sigma_2} = \frac{\phi + 1}{b\sigma_2 \phi}. \tag{B7}$$

To reach a certain total equilibrium population size ($\hat{n}_t$) the strenght of intra-specific competition (b) was standardized as follows

$$b = \frac{-1 - \phi}{n_t \phi} \cdot log\left(\frac{1}{\phi \sigma_2}\right). \tag{B8}$$

Given that the maximum growth rate λ_{max} could be calculated from

$$\lambda_{max} = \sqrt{\sigma_2 \phi}, \tag{B9}$$

life histories could be standardized for λ_{max} via ϕ adjustments as

$$\phi = \frac{\lambda_{max}^2}{\sigma_2}, \tag{B10}$$

such that the sensitivity $\partial \hat{n}_t / \partial \sigma_2$ could be generalized to

$$\frac{\partial \hat{n}_t}{\partial \sigma_2} = \frac{-n_t}{\sigma_2} \cdot log\left(\frac{1}{\lambda_{max}^2}\right)^{-1}. \tag{B11}$$

Rate of evolution at stable population size

To describe the rate of evolution we adapted equation 8 from Barfield et al. (2011) for our two-stage life cycle as

$$\Delta\bar{z} = G_2\ v_3\ w_2\ \sigma_2\ c\ \beta(z_2). \tag{B12}$$

The juvenile proportion could be derived from equation B3 and B5:

$$w_2 = \frac{\hat{n}_2}{\hat{n}_t} = \frac{\phi}{1+\phi}. \tag{B13}$$

The probability of surviving intra-specific competition (c) was derived by combining the Ricker function $c = exp(-bn_2)$ and equation B3:

$$c = exp(-bn_2) = \frac{1}{\phi\sigma_2}. \tag{B14}$$

The reproductive value of adults (v_3) could be derived from the left eigenvector (v) of the matrix population model (A) when solving $vA = \lambda v$ (Caswell, 2001, equation 4.81). For a population at equilibrium ($\lambda = 1$) the reproductive value of adults could be derived as

$$v_3 = \phi \tag{B15}$$

and normalized to

$$v_3 = \frac{1+\phi}{2} \tag{B16}$$

such that $v * w = 1$ (as in Barfield et al., 2011). The rate of evolution depending on the single vital rates

then could be expressed as

$$\Delta\bar{z} = \frac{1}{2}\, G_2 \beta(z_2) \tag{B17}$$

Appendix C: The standardization of life-history strategies

standardization

A critical aspect for the interpretation of our model and simulation results was the standardization of life-history strategies for uniform total population sizes $\hat{n}_t$ at stable conditions and for homogeneous maximum growth rates λ_{max} (also referred to as intrinsic rate of increase r). The population size standardization was necessary for two reasons. First, the environmental sensitivity $\partial n_t/\partial\sigma_2$ varied with the total population size (see equation 8), such that we had to measure it in the mathematical models at the same $\hat{n}_t$ to achieve informative comparisons between life histories. Second, the population size standardization allowed us to make $\partial n_t/\partial\sigma_2$ an informative proxy for extinction risk from short-term environmental variability. The population size reduction from environmental fluctuations determined the distance to critically low population sizes, the levels of genetic and demographic stochasticity, and thus fed back on survival during evolutionary rescue (Gomulkiewicz and Holt, 1995; Willi and Hoffmann, 2009; Lanfear et al., 2014; Carlson et al., 2014; Orive et al., 2017). While we are convinced that a population size standardization was necessary for this kind of study, we want to highlight that other kinds of standardization, for instance for the effective population size $\hat{n}_e$ (Caswell et al., 2004) or for uniform adult numbers $\hat{n}_3$, could make sense as well.

A life-history standardization for uniform maximum population growth rates was not mandatory, but highly useful. While the growth rate at population size equilibrium is always unity ($\lambda = 1$), the maximum population growth rate λ_{max} is an important demographic parameter with regard to a populations' recovery subsequent to detrimental environmental conditions (Lynch and Lande, 1993; Chevin et al., 2010). By running two sets of simulations with distinct levels of λ_{max} we could study the levels of robustness and evolvability not only along the axis of the fast-slow continuum (e.g., generation time T) but also along the axis of reproductive strategy as well (e.g., net reproductive rate R_0). This distinction revealed that the tradeoff between robustness and evolvability was only present when life histories with the same λ_{max} were compared to each other. Instead, both properties could be increased or decreased simultaneously when changes in vital rates translated into changes in λ_{max} (e.g., when moving to the bottom right or top-left corner in Fig. 2a). Thus, some life histories could be more evolvable and, at

the same time, more robust than others. We thus conclude that the described tradeoff is not a "hard" tradeoff but could be overcome, at least partly, by life-history evolution towards higher intrinsic growth rates (λ_{max}) along the reproductive strategy axis of life histories.

Two measures to quantify robustness against environmental variability

Even though we used two different robustness measures, $\partial\hat{n}_t/\partial\sigma_2$ and $\partial\lambda/\partial\sigma_2$, we suggest to not use them interchangeably given that they responded in opposite directions to some vital rate changes (see also Takada and Nakajima, 1998; Grant and Benton, 2000; Caswell et al., 2004). In our mathematical models, increasing a life history's maximum growth rate (e.g., to λ_{max}=1.15) resulted in a lower sensitivity of total population size ($\partial\hat{n}_t/\partial\sigma_2$) but in a higher sensitivity of the effective population size ($\partial\lambda/\partial\sigma_2$), such that one measure indicated an increase in robustness, and the other a decrease. Hence, it is unclear which measure is better suited to quantify a life history's robustness against interannual environmental fluctuations. On the one hand, $\partial\hat{n}_t/\partial\sigma_2$ was much better correlated to the extinction risk from short-term environmental variation than $\partial\lambda/\partial\sigma_2$ levels. On the other hand, this correlation might vanish, or even be reversed, when life-history strategies would have been standardized for the same 'effective' population size, instead of the same 'total' population size. We thus don't suggest to favor one measure over the other, but recommend a careful interpretation and further theoretical investigations.

References

Aitken, S. N., Yeaman, S., Holliday, J. a., Wang, T., and Curtis-McLane, S. (2008). Adaptation, migration or extirpation: Climate change outcomes for tree populations. Evolutionary Applications, 1(1):95–111.

Ancel, L. W. (2000). Undermining the Baldwin expediting effect: does phenotypic plasticity accelerate evolution? Theoretical Population Biology, 58(4):307–319.

Barfield, M., Holt, R. D., and Gomulkiewicz, R. (2011). Evolution in stage-structured populations. The American Naturalist, 177(4).

Beckman, N., Bullock, J. M., and Salguero-Gomez, R. (2018). High dispersal ability is related to fast life history strategies. Journal of Ecology, 106(March):1349–1362.

Bell, G. and Gonzalez, A. (2009). Evolutionary rescue can prevent extinction following environmental change. Ecology Letters, 12(9):942–948.

Boyce, M. S., Haridas, C. V., Lee, C. T., Boggs, C. L., Bruna, E. M., Coulson, T., Doak, D., Drake, J. M., Gaillard, J. M., Horvitz, C. C., Kalisz, S., Kendall, B. E., Knight, T., Mastrandrea, M., Menges, E. S., Morris, W. F., Pfister, C. A., and Tuljapurkar, S. D. (2006). Demography in an increasingly variable world. Trends in Ecology and Evolution, 21(3):141–148.

Brown, R. L. (2014). What evolvability really is. British Journal for the Philosophy of Science, 65(3):549–572.

Buoro, M. and Carlson, S. M. (2014). Life-history syndromes: Integrating dispersal through space and time. Ecology Letters, 17(6):756–767.

Bürger, R. (1999). Evolution of genetic variability and the advantage of sex and recombination in changing environments. Genetics, 153(2):1055–1069.

Bürger, R. and Lynch, M. (1995). Evolution and extinction in a changing environment: A quantitative-genetic analysis. Evolution, 49(1):151–163.

Carlson, S. M., Cunningham, C. J., and Westley, P. A. (2014). Evolutionary rescue in a changing world. Trends in Ecology and Evolution, 29(9):521–530.

Caswell, H. (2001). Matrix Population Models. Construction, Analysis, and Interpretation. Sinauer Associates, Inc., Sunderland, MA., 2nd edition.

Caswell, H., Takada, T., and Hunter, C. M. (2004). Sensitivity analysis of equilibrium in density-dependent matrix population models. Ecology Letters, 7(5):380–387.

Cayuela, H., Joly, P., Schmidt, B. R., Pichenot, J., Bonnaire, E., Priol, P., Peyronel, O., Laville, M., and Besnard, A. (2017). Life history tactics shape amphibians' demographic responses to the North Atlantic Oscillation. Global Change Biology, 23(11):4620–4638.

Charlesworth, B. (1994). Evolution in age-structured populations. Cambridge University Press, Cambridge, 2nd edition.

Chevin, L.-M., Cotto, O., and Ashander, J. (2017). Stochastic evolutionary demography under a fluctuating optimum phenotype. The American Naturalist, 190(6):000–000.

Chevin, L.-M., Lande, R., and Mace, G. M. (2010). Adaptation, plasticity, and extinction in a changing environment: Towards a predictive theory. PLoS Biology, 8(4):e1000357.

Cotto, O., Wessely, J., Georges, D., Klonner, G., Schmid, M., Dullinger, S., Thuiller, W., and Guillaume, F. (2017). A dynamic eco-evolutionary model predicts slow response of alpine plants to climate warming. Nature Communications, 8(May):15399.

Crother, B. I. and Murray, C. M. (2019). Early usage and meaning of evolvability. Ecology and Evolution, 9(7):3784–3793.

Dalgleish, H. J., Koons, D. N., and Adler, P. B. (2010). Can life-history traits predict the response of forb populations to changes in climate variability? Journal of Ecology, 98(1):209–217.

de Visser, J. A. G. M., Hermisson, J., Wagner, G. P., Meyers, L. A., Bagheri-Chaichian, H., Blanchard, J. L., Chao, L., Cheverud, J. M., Elena, S. F., Fontana, W., Gibson, G., Hansen, T. F., Krakauer, D., Lewontin, R. C., Ofria, C., Rice, S. H., von Dassow, G., Wagner, A., and Whitlock, M. C. (2003). Perspective: Evolution and detection of genetic robustness. Evolution, 57(9):1959.

Doak, D. F. and Morris, W. F. (2010). Demographic compensation and tipping points in climate-induced range shifts. Nature, 467(7318):959–962.

Duputié, A., Rutschmann, A., Ronce, O., and Chuine, I. (2015). Phenological plasticity will not help all species adapt to climate change. Global Change Biology, 21(8):3062–3073.

Ellner, S. P. and Hairston, N. G. (1994). Role of overlapping generations in maintaining genetic variation in a fluctuating environment. The American Naturalist, 143(3):403–417.

Engen, S., Lande, R., Sæther, B. E., and Weimerskirch, H. (2005). Extinction in relation to demographic and environmental stochasticity in age-structured models. Mathematical Biosciences, 195(2):210–227.

Engen, S., Sæther, B. E., Armitage, K. B., Blumstein, D. T., Clutton-Brock, T. H., Dobson, F. S., Festa-Bianchet, M., Oli, M. K., and Ozgul, A. (2013). Estimating the effect of temporally autocorrelated environments on the demography of density-independent age-structured populations. Methods in Ecology and Evolution, 4(6):573–584.

Evans, M. E. K. and Dennehy, J. J. (2005). Germ banking : Bet-hedging and variable release from egg and seed dormancy. The Quarterly Review of Biology, 80(4):431–451.

Falconer, D. S. and Mackay, T. F. C. (1996). Introduction to Quantitative Genetics. Pearson Prentice Hall, Harlow, Essex, UK, 4th edition.

Gaillard, J., Yoccoz, N. G., Lebreton, J., Bonenfant, C., Devillard, S., Loison, A., Pontier, D., and Allaine, D. (2005). Generation time: A reliable metric to measure life-history variation among mammalian populations. The American Naturalist, 166(1):119–123.

Gaillard, J.-M., Pontier, D., Allainé, D., Lebreton, J. D., Trouvilliez, J., and Clobert, J. (1989). An analysis of demographic tactics in birds and mammals. Oikos, 56(1):59–76.

Gomulkiewicz, R. and Holt, R. D. (1995). When does evolution by natural selection prevent extinction? Evolution, 49(1):201–207.

Grant, A. and Benton, T. G. (2000). Elasticity analysis for density-dependent populations in stochastic environments. Ecology, 81(3):680–693.

Guillaume, F. and Rougemont, J. (2006). Nemo: An evolutionary and population genetics programming framework. Bioinformatics, 22(20):2556–2557.

Hairston, N. G. and De Stasio Jr., B. T. (1988). Rate of evolution slowed by a dormant propagule pool. Nature, 336:239–242.

Hallett, L. M., Farrer, E. C., Suding, K. N., Mooney, H. A., and Hobbs, R. J. (2018). Tradeoffs in demographic mechanisms underlie differences in species abundance and stability. Nature Communications, 9(1):1–6.

Hansen, T. F., Solvin, T. M., and Pavlicev, M. (2019). Predicting evolutionary potential: A numerical test of evolvability measures. Evolution, 73(4):689–703.

Koons, D. N., Metcalf, C. J. E., and Tuljapurkar, S. (2008). Evolution of delayed reproduction in uncertain environments: A life-history perspective. The American Naturalist, 172(6):797–805.

Kopp, M. and Matuszewski, S. (2014). Rapid evolution of quantitative traits: Theoretical perspectives. Evolutionary Applications, 7(1):169–191.

Kuparinen, A., Savolainen, O., and Schurr, F. M. (2010). Increased mortality can promote evolutionary adaptation of forest trees to climate change. Forest Ecology and Management, 259(5):1003–1008.

Lande, R. (1982). A quantitative genetic theory of life history evolution. Ecology, 63(3):607–615.

Lande, R. (1993). Risks of population extinction from demographic and environmental stochasticity and random catastrophes. The American Naturalist, 142(6):911–927.

Lande, R. and Orzack, S. H. (1988). Extinction dynamics of age-structured populations in a fluctuating environment. Proceedings of the National Academy of Sciences of the United States of America, 85(19):7418–21.

Lanfear, R., Kokko, H., and Eyre-Walker, A. (2014). Population size and the rate of evolution. Trends in Ecology and Evolution, 29(1):33–41.

Lynch, M., Gabriel, W., and Wood, A. M. (1991). Adaptive and demographic responses of plankton populations to environmental change. Limnology and Oceanography, 36(7):1301–1312.

Lynch, M. and Lande, R. (1993). Evolution and extinction in response to environmental change. In Biotic Interactions and Global Change, pages pp. 234–250.

Marshall, D. J., Burgess, S. C., and Connallon, T. (2016). Global change, life-history complexity and the potential for evolutionary rescue. Evolutionary Applications, 9(9):1189–1201.

Mayer, C. and Hansen, T. F. (2017). Evolvability and robustness: A paradox restored. Journal of Theoretical Biology, 430:78–85.

McDonald, J. L., Franco, M., Townley, S., Ezard, T. H., Jelbert, K., and Hodgson, D. J. (2017). Divergent demographic strategies of plants in variable environments. Nature Ecology and Evolution, 1(2).

Metcalf, C. J. E. and Pavard, S. (2007). Why evolutionary biologists should be demographers. Trends in Ecology and Evolution, 22(4):205–212.

Morris, W. F., Pfister, C. A., Tuliapurkar, S., Haridas, C. V., Boggs, C. L., Boyce, M. S., Bruna, E. M., Church, D. R., Coulson, T., Doak, D. F., Forsyth, S., Gaillard, J.-m., Horvitz, C. C., Kalisz, S., Kendall, B. E., Knight, T. M., Lee, C. T., Menges, E. S., Chirrakal, V., Boggs, C. L., Boyce, M. S., Bruna, E. M., Church, D. R., Coulson, T., Doak, D. F., Forsyth, S., Gaillard, J.-m., Horvitz, C. C., Kalisz, S., Kendall, E., Knight, T. M., Lee, C. T., and Menges, E. S. (2008). Longevity can buffer plant and animal populations against changing climatic variability. Ecology, 89(1):19–25.

Neubert, M. G. and Caswell, H. (2000). Density-dependent vital rates and their population dynamic consequences. Journal of Mathematical Biology, 121(34):103–121.

Orive, M. E., Barfield, M., Fernandez, C., and Holt, R. D. (2017). Effects of clonal reproduction on evolutionary lag and evolutionary rescue. The American Naturalist, 190(4).

Orzack, S. H. and Tuljapurkar, S. D. (1989). Population Dynamics in Variable Environments . VII . The Demography and Evolution of Iteroparity. The American Naturalist, 133(6):901–923.

Osmond, M. M., Otto, S. P., and Klausmeier, C. A. (2017). When predators help prey adapt and persist in a changing environment. The American Naturalist, 190(1):000–000.

Paniw, M., Ozgul, A., and Salguero-Gómez, R. (2017). Interactive life-history traits predict sensitivity of plants and animals to temporal autocorrelation. Ecology Letters, pages 275–286.

Parmesan, C. (2006). Ecological and evolutionary responses to recent climate change. Annual Review of Ecology, Evolution, and Systematics, 37(1):637–669.

Payne, J. L. and Wagner, A. (2018). The causes of evolvability and their evolution. Nature Reviews Genetics.

Petit, R. J. and Hampe, A. (2006). Some evolutionary consequences of being a tree. Annual Review of Ecology, Evolution, and Systematics, 37(May):187–214.

Pigliucci, M. (2008). Is evolvability evolvable? Nature Reviews Genetics, 9(1):75–82.

R Development Core Team (2008). R: a language and environment for statistical computing.

Sæther, B.-E., Coulson, T., Grøtan, V., Engen, S., Altwegg, R., Armitage, K. B., Barbraud, C., Becker, P. H., Blumstein, D. T., Dobson, F. S., Festa-Bianchet, M., Gaillard, J.-M., Jenkins, A., Jones, C., Nicoll, M. A. C., Norris, K., Oli, M. K., Ozgul, A., and Weimerskirch, H. (2013). How life history influences population dynamics in fluctuating environments. The American Naturalist, 182(6):743–759.

Salguero-Gómez, R. (2017). Applications of the fast–slow continuum and reproductive strategy framework of plant life histories. New Phytologist, 213(4):1618–1624.

Salguero-Gómez, R., Jones, O. R., Blomberg, S. P., Hodgson, D. J., Zuidema, P. A., and Kroon, H. D. (2017). Fast–slow continuum and reproductive strategies structure plant life-history variation worldwide. Proceedings of the National Academy of Sciences, 114(45):E9753–E9753.

Sasaki, A. and Ellner, S. (1997). Quantitative genetic variance maintained by fluctuating selection with overlapping generations : Variance components and covariances. Evolution, 51(3):682–696.

Stearns, S. C. (1983). The influence of size and phylogeny on patterns of covariation among life-history traits in the mammals. Oikos, 41(2):173–187.

Stocker, T., Qin, D., Plattner, G.-K., Tignor, M., Allen, S., Boschung, J., Nauels, A., Xia, Y., Bex, V., and Midgley, P. (2013). IPCC, 2013: Climate Change 2013: The Physical Science Basis. Contribution of Working Group I to the Fifth Assessment Report of the Intergovernmental Panel on Climate Change. Technical report, IPCC, Cambridge University Press, Cambridge, United Kingdom and New York, NY, USA.

Stubben, C. J. and Milligan, B. G. (2007). Estimating and Analyzing Demographic Models Using the popbio Package in R. Journal of Statistical Software, 22:11.

Sumedha, Martin, O. C., and Wagner, A. (2007). New structural variation in evolutionary searches of RNA neutral networks. BioSystems, 90(2):475–485.

Svardal, H., Rueffler, C., and Hermisson, J. (2015). A general condition for adaptive genetic polymorphism in temporally and spatially heterogeneous environments. Theoretical Population Biology, 99:76–97.

Takada, T. and Nakajima, H. (1998). Theorems on the invasion process in stage-structured populations with density-dependent dynamics. Journal of Mathematical Biology, 36(5):497–514.

Templeton, A. R. and Levin, D. A. (1979). Evolutionary consequences of seed pools. The American Naturalist, 114(2):232–249.

Tuljapurkar, S., Gaillard, J. M., and Coulson, T. (2009). From stochastic environments to life histories and back. Philosophical Transactions of the Royal Society B: Biological Sciences, 364(1523):1499–1509.

Tuljapurkar, S. D. (1982). Population dynamics in variable environments. III. Evolutionary dynamics of r-selection. Theoretical Population Biology, 21:141–165.

Tuljapurkar, S. D. (1990). Population Dynamics in Variable Environments. Springer Verlag, Berlin Heidelberg.

Ummenhofer, C. C. and Meehl, G. A. (2017). Extreme weather and climate events with ecological relevance: a review. Philosophical Transactions of the Royal Society B: Biological Sciences, 372(1723):20160135.

Van De Pol, M., Vindenes, Y., Sæther, B. E., Engen, S., Ens, B. J., Oosterbeek, K., and Tinbergen, J. M. (2010). Effects of climate change and variability on population dynamics in a long-lived shorebird. Ecology, 91(4):1192–1204.

Vander Wal, E., Garant, D., Festa-Bianchet, M., and Pelletier, F. (2013). Evolutionary rescue in vertebrates: Evidence, applications and uncertainty. Philosophical Transactions of the Royal Society B: Biological Sciences, 368(1610).

Vázquez, D. P., Gianoli, E., Morris, W. F., and Bozinovic, F. (2015). Ecological and evolutionary impacts of changing climatic variability. Biological Reviews, 92:22–42.

Via, S. and Lande, R. (1985). Genotype-environment interaction and the evolution of phenotypic plasticity. Evolution, 39(3):505–522.

Wagner, A. (2008). Robustness and evolvability: A paradox resolved. Proceedings of the Royal Society B: Biological Sciences, 275(1630):91–100.

Willi, Y. and Hoffmann, A. A. (2009). Demographic factors and genetic variation influence population persistence under environmental change. Journal of Evolutionary Biology, 22(1):124–133.

Yamamichi, M., Jr, N. G. H., Rees, M., and Ellner, S. P. (2019). Rapid evolution with generation overlap : The double-edged effect of dormancy. Theoretical Ecology, 12(2):179–195.

Zeineddine, M. and Jansen, V. A. A. (2009). To age, to die: Parity, evolutionary tracking and Cole's paradox. Evolution, 63(6):1498–1507.

Supplementary Material

Supp A: 3-stage model with Beverton-Holt density regulation

Equilibrium population size

The demographic dynamics were modeled via the population vector

$$N = \begin{pmatrix} n_1 \\ n_2 \\ n_3 \end{pmatrix} \tag{S1}$$

and the MPM

$$A = \begin{bmatrix} \sigma_1(1-\gamma) & 0 & \phi \\ \sigma_1(\gamma) & 0 & 0 \\ 0 & \sigma_2 \cdot 1/(1+bn_3) & \sigma_3 \end{bmatrix} \tag{S2}$$

such that $N(t+1) = AN(t)$. At equilibrium $\hat{N} = A\hat{N}$ with $\hat{N} = c(\hat{n}_1, \hat{n}_2, \hat{n}_3)^T$. The number of offspring, juveniles, and adults at equilibrium then could be derived as

$$\hat{n}_1 = \frac{\phi}{b(1-\sigma_1(1-\gamma))} \cdot \left(\frac{\sigma_2\sigma_1\gamma\phi}{(1-\sigma_3)(1-\sigma_1(1-\gamma))} - 1 \right), \tag{S3}$$

$$\hat{n}_2 = \frac{\phi\sigma_1\gamma}{b(1-\sigma_1(1-\gamma))} \left(\frac{\sigma_2\sigma_1\gamma\phi}{(1-\sigma_3)(1-\sigma_1(1-\gamma))} - 1 \right), \tag{S4}$$

$$\hat{n}_3 = \frac{1-\sigma_1(1-\gamma)}{b(1-\sigma_1(1-\gamma))} \cdot \left(\frac{\sigma_2\sigma_1\gamma\phi}{(1-\sigma_3)(1-\sigma_1(1-\gamma))} - 1 \right). \tag{S5}$$

The total population size at equilibrium was computed from $\hat{n}_t = \hat{n}_1 + \hat{n}_2 + \hat{n}_3$ as

$$\hat{n}_t = \frac{\phi + \phi\sigma_1\gamma + 1 - \sigma_1(1-\gamma)}{b(1-\sigma_1(1-\gamma))} \cdot \left(\frac{\sigma_2\sigma_1\gamma\phi}{(1-\sigma_3)(1-\sigma_1(1-\gamma))} - 1 \right). \tag{S6}$$

Sensitivity of total population size to juvenile survival

The partial derivative of the total population size at equilibrium ($\hat{n}_t$) to juvenile survival (σ_2) was calculated as

$$\frac{\partial \hat{n}_t}{\partial \sigma_2} = \frac{\phi + \phi\sigma_1\gamma + 1 - \sigma_1(1-\gamma)}{b(1-\sigma_1(1-\gamma))} \cdot \left(\frac{\sigma_1\gamma\phi(1-\sigma_3)(1-\sigma_1(1-\gamma) - 0}{((1-\sigma_3)(1-\sigma_1(1-\gamma))^2} - 0) \right) \tag{S7}$$

and could be simplified to

$$\frac{\partial \hat{n}_t}{\partial \sigma_2} = \frac{\phi + \phi\sigma_1\gamma + 1 - \sigma_1(1-\gamma)}{b(1-\sigma_1(1-\gamma))} \cdot \left(\frac{\sigma_1\gamma\phi}{(1-\sigma_3)(1-\sigma_1(1-\gamma))} \right). \tag{S8}$$

To reach a certain total equilibrium population size ($\hat{n}_t$) the strenght of intra-specific competition can be standardized as follows

$$b = \frac{\phi + \phi\sigma_1\gamma + 1 - \sigma_1(1-\gamma)}{\hat{n}_t(1-\sigma_1(1-\gamma))} \cdot \left(\frac{\sigma_2\sigma_1\gamma\phi}{(1-\sigma_3)(1-\sigma_1(1-\gamma))} - 1 \right). \tag{S9}$$

By inserting equation S9 in S8 the population size sensitivity to juvenile survival could be standardized for $\hat{n}_t$ as

$$\begin{aligned} \frac{\partial \hat{n}_t}{\partial \sigma_2} = & \frac{\phi + \phi\sigma_1\gamma + 1 - \sigma_1(1-\gamma)}{(1-\sigma_1(1-\gamma))} \cdot \left(\frac{\sigma_1\gamma\phi}{(1-\sigma_3)(1-\sigma_1(1-\gamma))} \right) \cdot \\ & \frac{\hat{n}_t(1-\sigma_1(1-\gamma))}{\phi + \phi\sigma_1\gamma + 1 - \sigma_1(1-\gamma)} \cdot \left(\frac{(1-\sigma_3)(1-\sigma_1(1-\gamma))}{\sigma_2\sigma_1\gamma\phi - (1-\sigma_3)(1-\sigma_1(1-\gamma))} \right), \end{aligned} \tag{S10}$$

such that the following partial derivative is obtained

$$\frac{\partial \hat{n}_t}{\partial \sigma_2} = \frac{\hat{n}_t \sigma_1 \gamma \phi}{\sigma_2 \sigma_1 \gamma \phi - (1-\sigma_3)(1-\sigma_1(1-\gamma))}, \tag{S11}$$

Rate of evolution at stable population size

The equation from Barfield et al. (2011) could be adapted for our 3-stage life cycle as

$$\Delta \bar{z} = w_2 \ \sigma_2 \ c \ v_3 \ G_2 \beta(z_2). \tag{S12}$$

The juvenile proportion (w_2) can be derived from equation S4 and A6 as

$$w_2 = \frac{\hat{n}_2}{\hat{n}_t} = \frac{\phi \sigma_1 \gamma}{\phi + \sigma_1 \gamma(\phi+1) - \sigma_1 + 1}. \tag{S13}$$

The probability of surviving intra-specific competition (c) can be derived by combining the Beverton-Holt function $c = 1/(1 + bn_3)$ and equation S5

$$c = \frac{(1-\sigma_3)(1-\sigma_1(1-\gamma))}{\sigma_2 \sigma_1 \gamma \phi} \tag{S14}$$

The reproductive value of adults (v_3) can be derived from the left eigenvector (v) of the matrix population model (A) when solving $v^T A = \lambda v^T$ (Caswell 2001, chapter 4.6, equation 4.81). For a population at its stable population size ($\lambda = 1$) the reproductive value of adults is

$$v_3 = \frac{\phi}{(1-\sigma_3)} \tag{S15}$$

The normalization of v_3 such that $v^T w = 1$ could be achieved as

$$v_3 = \frac{\phi + \sigma_1 \gamma(\phi+1) - \sigma_1 + 1}{(1-\sigma_3)(1-\sigma_1(1-\gamma) + (1-\sigma_3) + (1-\sigma_1(1-\gamma))} \tag{S16}$$

The rate of evolution then can be expressed as

$$\Delta\bar{z} = \frac{(1-\sigma_3)(1-\sigma_1(1-\gamma)}{(1-\sigma_3)(1-\sigma_1(1-\gamma)+(1-\sigma_3)+(1-\sigma_1(1-\gamma))}\ G_2\beta(z_2) \tag{S17}$$

Supp B: 2-stage model with Beverton-Holt density regulation

Equilibrium population size

Population dynamics were modeled with the population vector

$$N = \begin{pmatrix} n_2 \\ n_3 \end{pmatrix} \tag{B1}$$

and the matrix population model

$$A = \begin{bmatrix} 0 & \phi \\ \dfrac{\sigma_2}{(1+bn_2)} & 0 \end{bmatrix} \tag{B2}$$

such that $N(t+1) = An$ with equilibrium $\hat{N} = A\hat{N}$.

The number of juveniles and adults at equilibrium then could be derived as

$$\hat{n}_2 = \frac{\phi(\phi\sigma_2 - 1)}{b\phi}, \tag{B3}$$

and

$$\hat{n}_3 = \frac{\phi\sigma_2 - 1}{b\phi}, \tag{B4}$$

with a total population size at equilibrium of

$$\hat{n}_t = \frac{(\phi+1)(\phi\sigma_2 - 1)}{b\phi}. \tag{B5}$$

Sensitivity of total population size to juvenile survival

The partial derivative of the total population size at equilibrium ($\hat{n}_t$) with respect to juvenile survival (σ_2) can be computed as

$$\frac{\partial \hat{n}_t}{\partial \sigma_2} = \frac{b\phi \cdot (\phi(\phi+1) - 0}{(b\phi)^2}, \tag{B6}$$

and simplified to

$$\frac{\partial \hat{n}_t}{\partial \sigma_2} = \frac{\phi(\phi+1)}{b\phi}. \tag{B7}$$

The strength of intra-specific competition (b) could be standardized to reach a certain equilibrium population size ($\hat{n}_t$) via

$$b = \frac{(\phi+1)(\phi\sigma_2 - 1)}{n_t\phi}, \tag{B8}$$

while the fecundity (ϕ) could be used to standardize a life history for a specific maximum growth rate (λ_{max}) when

$$\lambda_1 = \sqrt{\sigma_2\phi}, \tag{B9}$$

and

$$\phi = \frac{\lambda_1^2}{\sigma_2}. \tag{B10}$$

The sensitivity $\partial\hat{n}_t/\partial\sigma_2$ then could be reformulated as

$$\frac{\partial \hat{n}_t}{\partial \sigma_2} = \frac{\hat{n}_t}{\sigma_2} \cdot \frac{\lambda_1^2}{(\lambda_1^2 - 1)}. \tag{B11}$$

Rate of evolution at stable population size

The equation from Barfield et al. (2011) can be adapted for our two-stage life cycle as

$$\Delta\bar{z} = w_2 \ \sigma_2 \ c \ v_3 \ G_2\beta(z_2). \tag{B12}$$

The juvenile proportion can be derived from equation B3 and B5:

$$w_2 = \frac{\hat{n}_2}{\hat{n}_t} = \frac{\phi}{1+\phi}, \tag{B13}$$

and the probability of surviving intra-specific competition (c) can be derived by combining the Beverton-Holt function $c = 1/(1 + b\hat{n}_2)$ and equation B3:

$$c = 1/(1 + b\hat{n}_2) = \frac{1}{\phi\sigma_2}. \tag{B14}$$

The reproductive value of adults for the 2-stage life history with Beverton-Holt density regulation is

$$v_3 = \phi \tag{B15}$$

and can be normalize ($v^T w = 1$) to

$$v_3 = \frac{1+\phi}{2}. \tag{B16}$$

The rate of evolution for two-stage life history at population size equilibrium with BH density regulation then can be expressed as

$$\Delta\bar{z} = \frac{1}{2} \ G_2\beta(z_2). \tag{B17}$$

Supp C: Plots mathematical model

Figure S1: 3 stages (standardized for $n_t + \lambda_{max}$)

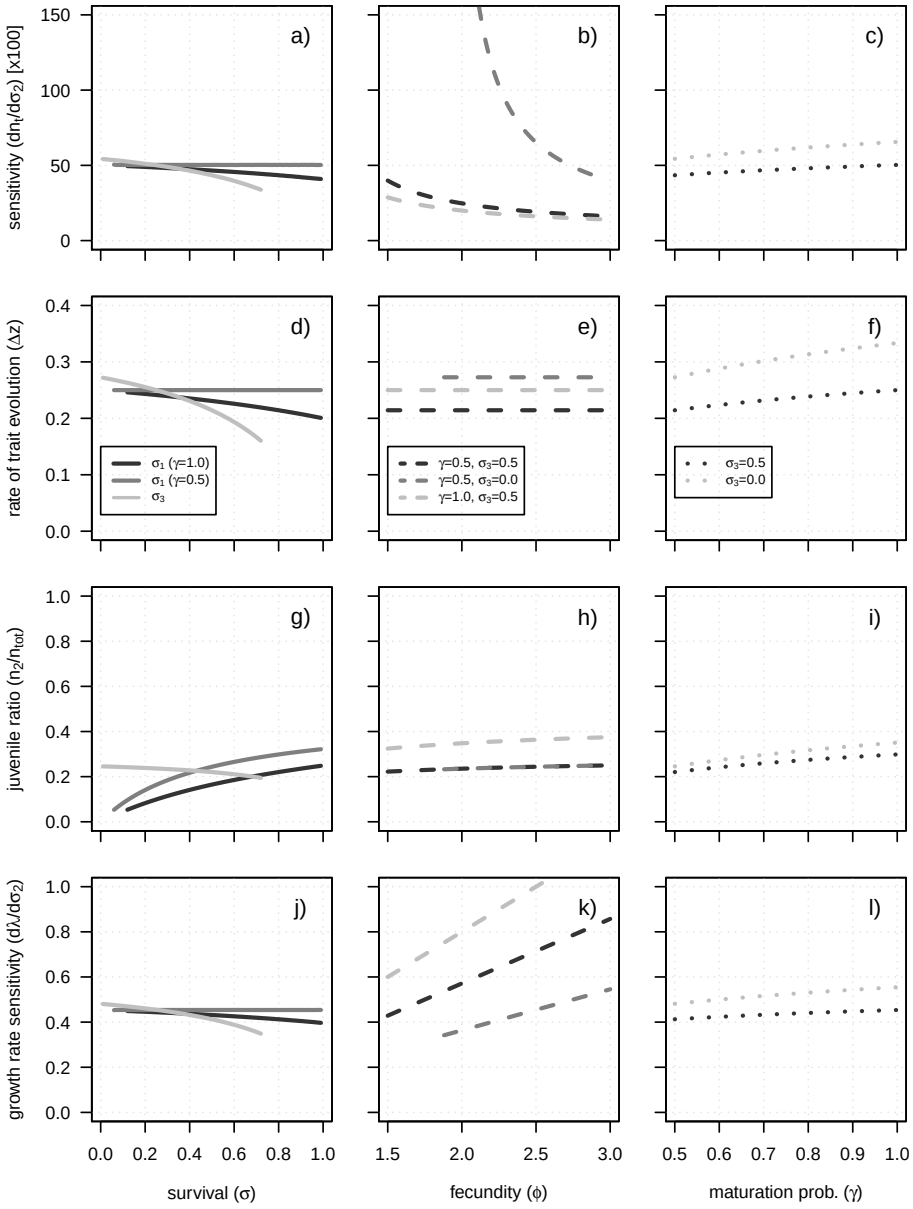

Figure S1: The model results for the sensitivity of the total population size ($\partial\hat{n}_t/\partial\sigma_2$, a-c), the rate of evolution (Δz, d-f), the juvenile ratio ($\hat{n}_2/\hat{n}_t$, g-i), and the sensitivity of the max. growth rate ($\partial\lambda/\partial\sigma_2$, j-l) are shown depending on a life histories' survival rate (σ_1,σ_3), fecundity (ϕ), and maturation probability (γ). The maximum growth rate has been standardized for $\lambda_{max} = 1.1$ by fecundity adjustments, except for the case when we varied fecundity (b,e,h,k). Each parameter combination has been standardized for the same equilibrium population size in absence of interannual environmental fluctuations ($\hat{n}_t$=1500) via adjustments of the strength of competition (**b**). The following parameter values have been used if not other specified: $\sigma_1 = 0.8$, $\sigma_2 = 0.8$, $\sigma_3 = 0.5$, $\gamma = 0.5$, $G = 1$, and $\beta(z_2) = 1$. This graph is identical to figure 3 but shows additionally the juvenile ratio.

Figure S2: 2 stages (standardized for $n_t + \lambda_{max}$)

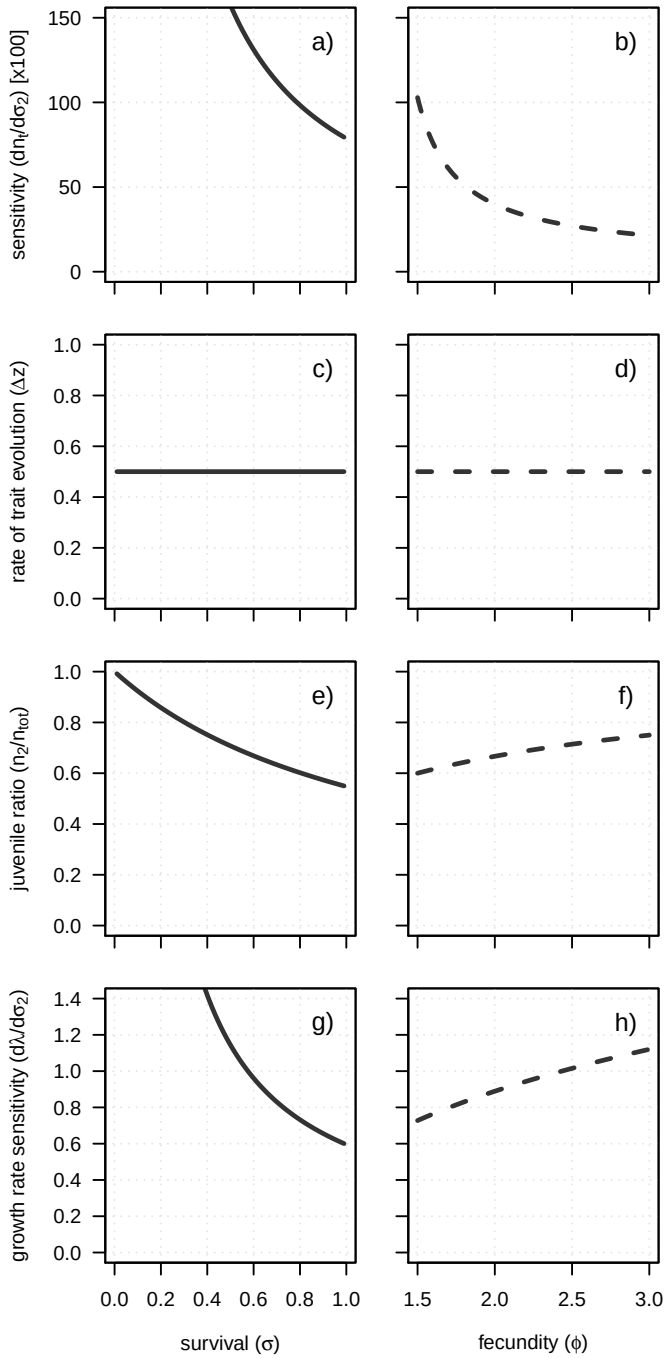

Figure S2: The sensitivity of the total population size ($\partial\hat{n}_t/\partial\sigma_2$, a-b), the rate of evolution (Δz, c-d), the juvenile ratio ($\hat{n}_2/\hat{n}_t$, e-f), and the sensitivity of the max. growth rate ($\partial\lambda/\partial\sigma_2$, g-h) are shown depending on the two-stage life cycles' survival rate (σ_2) and fecundity (ϕ). The maximum growth rate has been standardized for $\lambda_{max} = 1.1$ by fecundity adjustments, except for the case when we varied fecundity (b,d,f,h). Each parameter combination has been standardized for the same equilibrium population size in absence of interannual environmental fluctuations ($\hat{n}_t$=1500) via adjustments of the strength of competition (**b**). , $G = 1$, and $\beta(z_2) = 1$

Figure S3: 3 stages (standardized for n_t only)

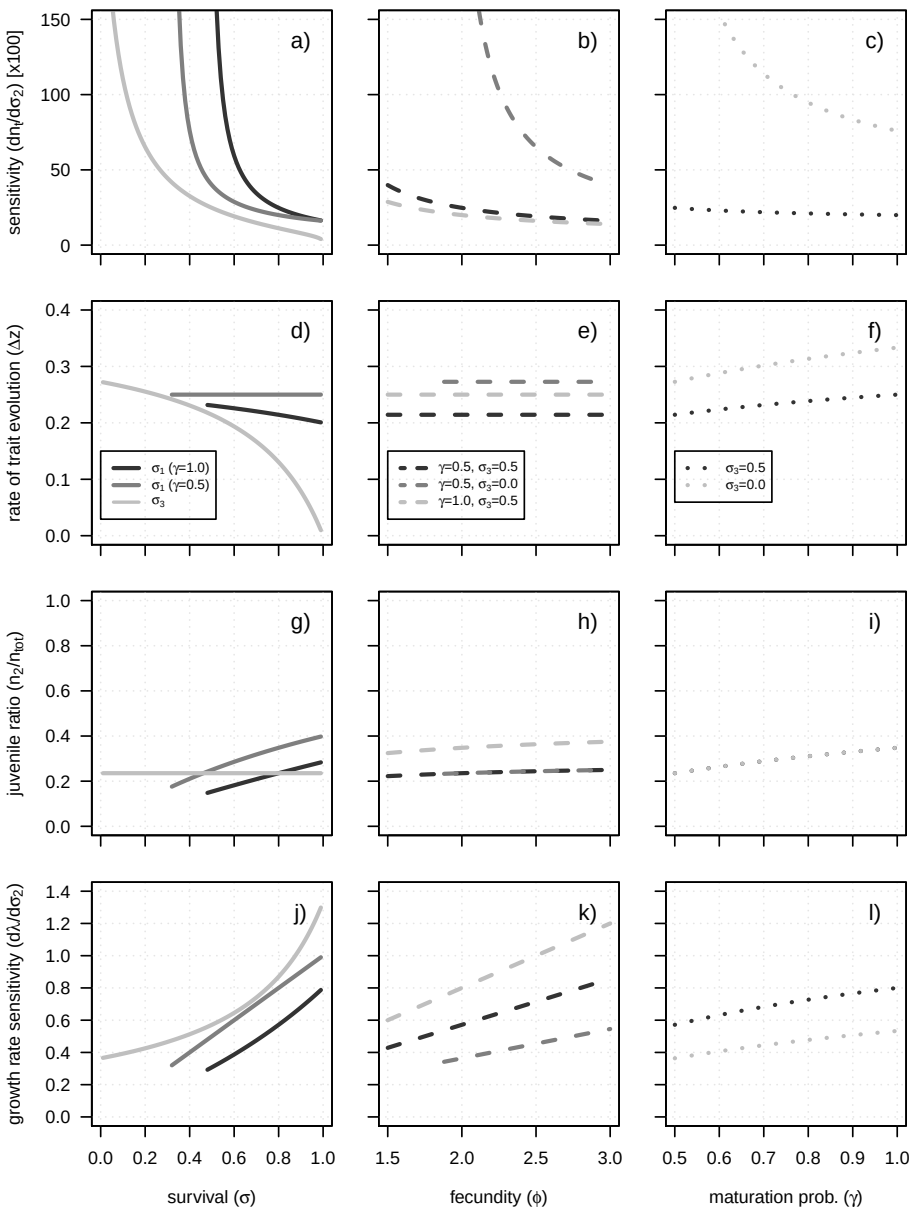

Figure S3: The model results for three-stage life cycles are shown for the sensitivity of the total population size ($\partial\hat{n}_t/\partial\sigma_2$, a-c), the rate of evolution (Δz, d-f), the juvenile ratio ($\hat{n}_2/\hat{n}_t$, g-i), and the sensitivity of the max. growth rate ($\partial\lambda/\partial\sigma_2$, j-l) depending on a life histories' survival rate (σ_1,σ_3), fecundity (ϕ), and maturation probability (γ). Each parameter combination has been standardized for the same equilibrium population size in absence of interannual environmental fluctuations ($\hat{n}_t$=1500) via adjustments of the strength of competition (**b**). However, the maximum growth rate has NOT been standardized in this case. The following parameter values have been used if not other specified: $\sigma_1 = 0.8$, $\sigma_2 = 0.8$, $\sigma_3 = 0.5$, $\phi = 2$, $G = 1$, and $\beta(z_2) = 1$. This figure shows the same results as figure 3 but adds the proportion of juveniles (g-i).

Figure S4: 2 stages (standardized for n_t only)

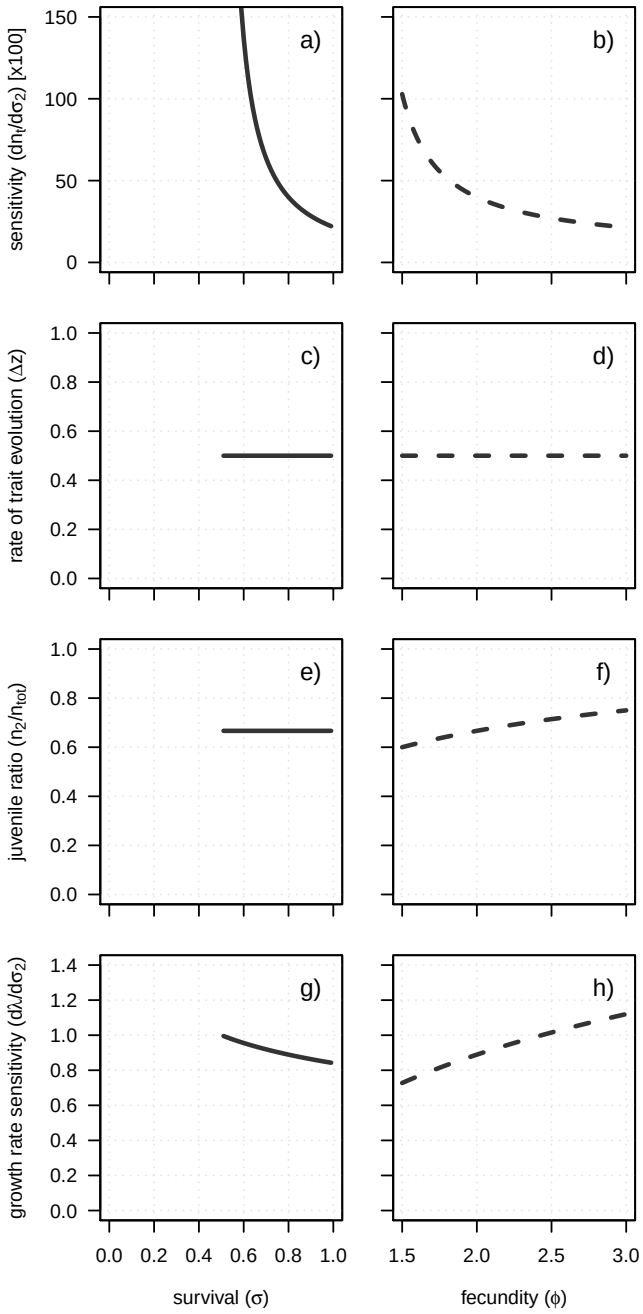

Figure S4: The model results for two-stage life cycles illustrate the sensitivity of the total population size ($\partial\hat{n}_t/\partial\sigma_2$, a-b), the rate of evolution (Δz, c-d), the juvenile ratio ($\hat{n}_2/\hat{n}_t$, e-f), and the sensitivity of the max. growth rate ($\partial\lambda/\partial\sigma_2$, g-h) depending on a life histories' survival rate (σ_2) and fecundity (ϕ). Each parameter combination has been standardized for the same equilibrium population size in absence of interannual environmental fluctuations ($\hat{n}_t$=1500) via adjustments of the strength of competition (**b**). However, the maximum growth rate has NOT been standardized for $\lambda_{max} = 1.1$ by fecundity adjustments. Juvenile survival was fixed to $\sigma_2 = 0.8$ with varying fecundity (b,d,f,h) and fecundity was set to $\phi = 2$ with varying σ_2 (a,c,e,g).

Figure S5: evolvability-robustness tradeoff with Beverton-Holt density regulation

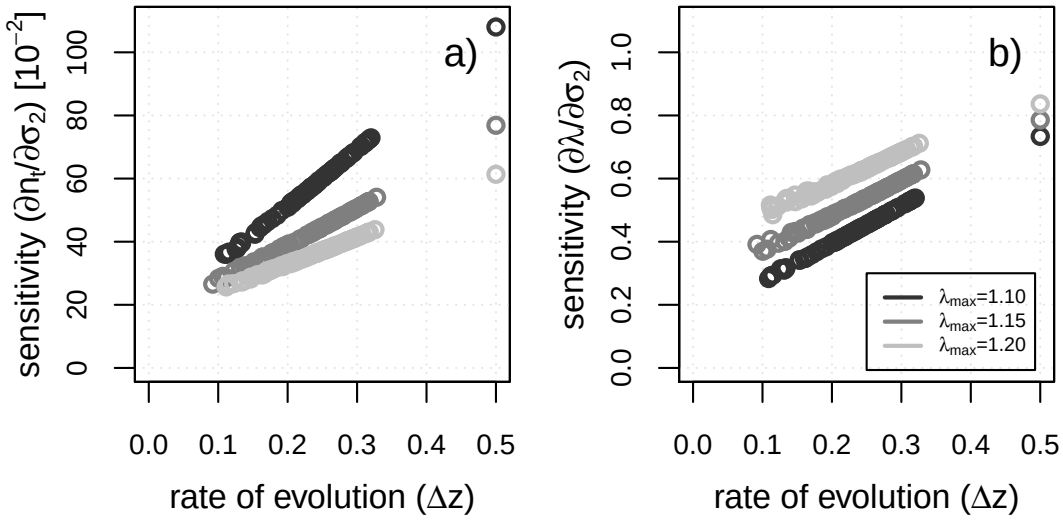

Figure S5: A life history's tradeoff between evolvability (Δz) and robustness ($\partial \hat{n}_t/\partial \sigma_2$ in a, and $\partial \lambda/\partial \sigma_2$ in b) using a Beverton-Holt function for density regulation. Each circle illustrates a random combination of vital rates (with $0.2 \leq \sigma_1 \leq 1.0$, $\sigma_2 = 0.8$, $0.0 \leq \sigma_3 \leq 0.9$, $0.2 \leq \gamma \leq 1.0$). The fecundity (ϕ) and the strength of competition (b) were re-calculated for each vital rate combination to standardize the maximum population growth rate ($\lambda_{max} = 1.10 - black, \lambda_{max} = 1.15 - darkgray, \lambda_{max} = 1.20 - lightgray$) and the total population size at stable conditions (n_t=1'500). We then calculated the rate of evolution (Δz, with $G_2\beta(z_2) = 1$), the population size sensitivity ($\partial \hat{n}_t/\partial \sigma_2$), and the growth rate sensitivity ($\partial \lambda/\partial \sigma_2$) for each life-history variant. The three single points on the right of the plots were derived for the 2-stage life cycle (with $\sigma_2 = 0.8$), while the rest of the points illustrate parameter combinations for 3-stage life cycles.

Figure S6: compare results for Δz, $\partial \hat{n}_t/\partial \sigma_2$, and $\partial \lambda/\partial \sigma_2$ between models with Beverton-Holt and Ricker density regulation

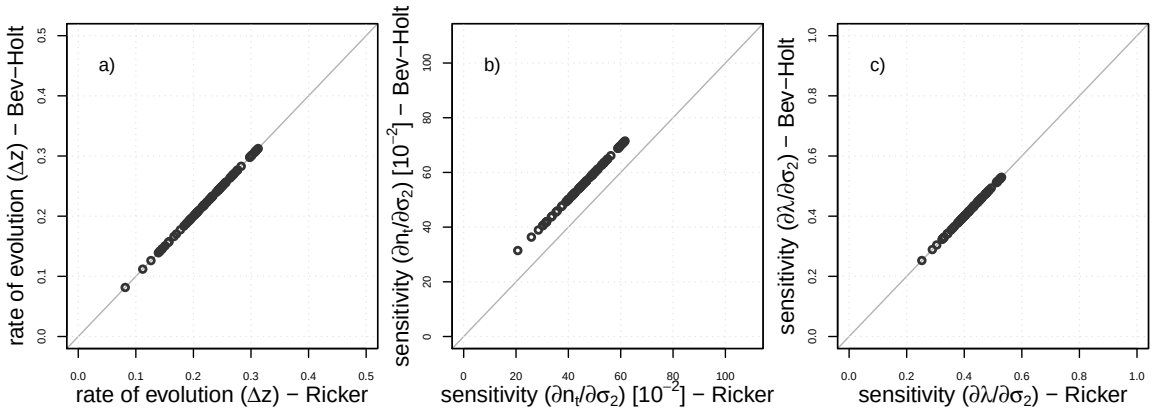

Figure S6: These graphs compare the model results for density regulation based on the Ricker function with the models based on the Beverton-Holt function, contrasting the rate of evolution (Δz), the sensitivity of the total population size to juvenile survival ($\partial \hat{n}_t/\partial \sigma_2$), and the sensitivity of the population growth rate to juvenile survival ($\partial \lambda/\partial \sigma_2$). Each dot is a random combination of vital rates with $0.2 \leq \sigma_1 \leq 1.0$, $\sigma_2 = 0.8$, $0.0 \leq \sigma_3 \leq 0.9$, $0.2 \leq \gamma \leq 1.0$.

Figure S7: Population growth over time for all four life histories and both levels of λ_{max}

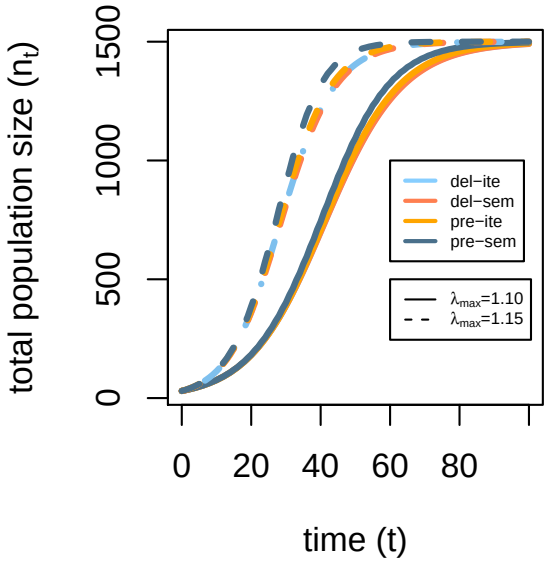

Figure S7: This graph illustrates the growth trajectories for all four life histories (*del-ite*, *del-sem*, *pre-sem*, *pre-ite*) and both maximum growth rates ($\lambda_{max} = 1.10$ and $\lambda_{max} = 1.15$) over time. All life histories here start at the same total population size ($n_t = 30$) and grow to the same carrying capacity of 1500 individuals ($n_t = n_1 + n_2 + n_3$). The population growth trajectories are quite similar across life histories with the same λ_{max}, while $\lambda_{max} = 1.15$ results in a faster increase in n_t than a standardization for $\lambda_{max} = 1.10$. In the beginning, stage structure was adjusted to the SSD of the respective life history.

Supp D: Plots individual-based simulations

Figure S8: Evolution of G_2 with $\lambda = 1.15$

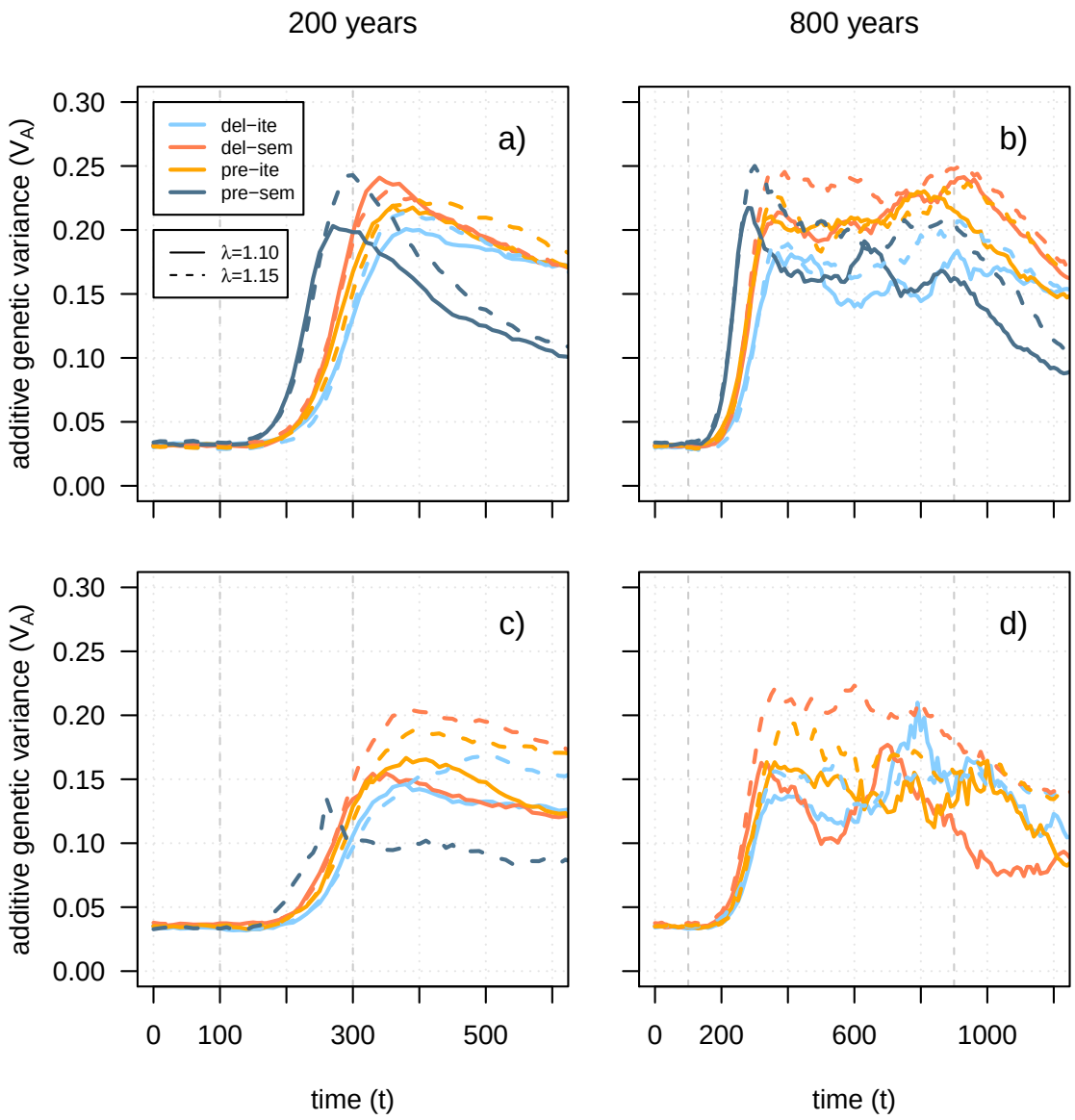

Figure S8: Simulation results for the evolution of additive genetic variance during environmental change are shown for the four life histories, the two different duration of environmental change (200 years - a,c; 800 years - b,d) and two degrees of interannual environmental variability ($\epsilon = 0.2$ - a,b; $\epsilon = 1.0$ - c,d). The simulation results were averaged over all of the 100 replicates that did not went extinct.

Figure S9: Extinction dynamics with $\lambda = 1.15$

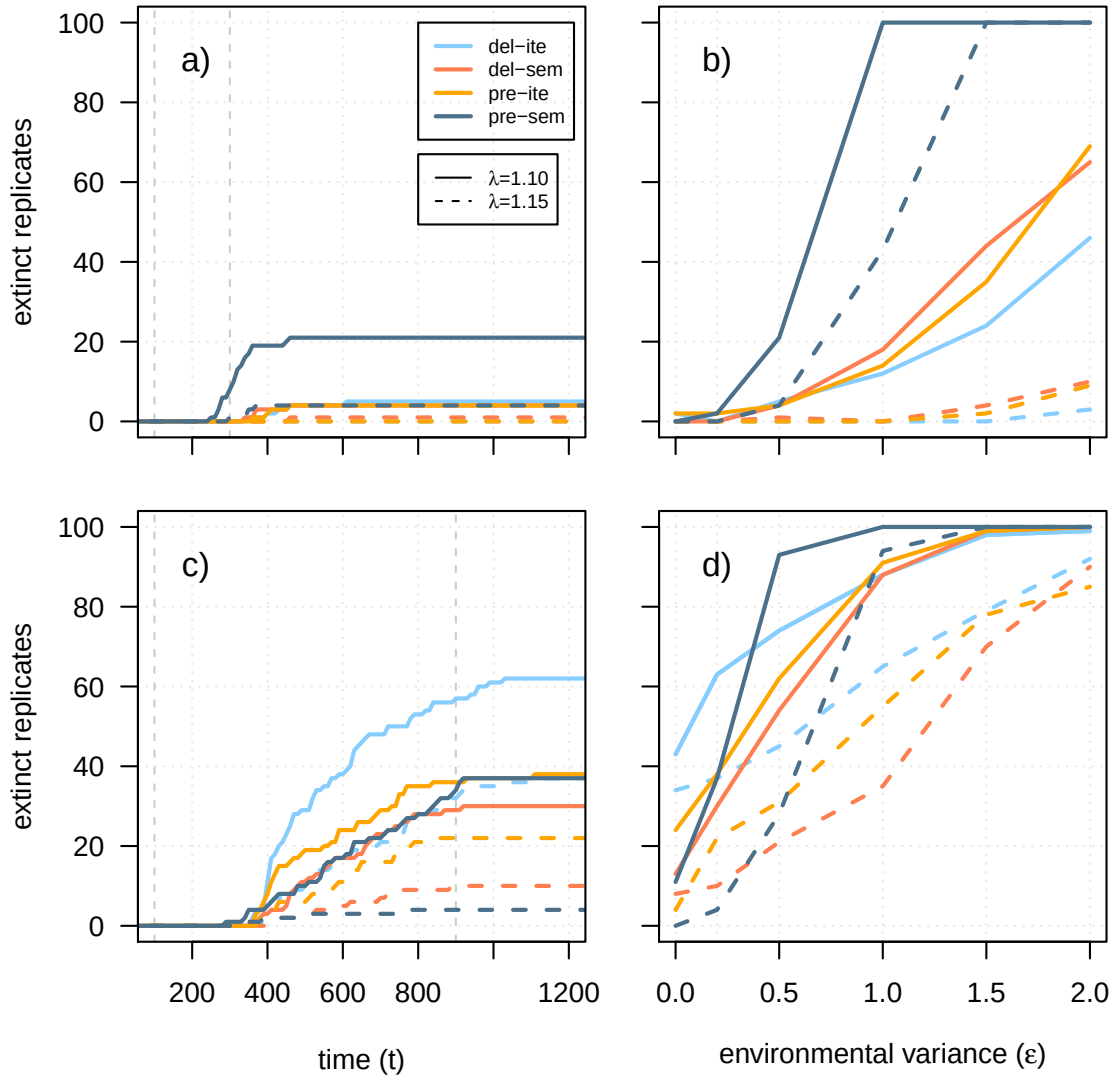

Figure S9: These graphs show the same simulation results on the number of extinct replicates as figure 6, but illustrate additionally the results for the life-history standardization of $\lambda_{max} = 1.15$. These graphs show for each of the four life histories the number of extinct replicates over time t (a,c) and the total number of extinct replicates depending on environmental variability ϵ (b,d). Extinction dynamics are shown for two different scenarios with environmental change either lasting for 200 years (a,b) or for 800 years (c,d). The gray dashed lines indicate the start of environmental change ($t = 100$) and its end ($t = 300$ for a,b; $t = 900$ for c,d). In both scenarios, the rate of environmental change per year was set to $\Delta\bar{\theta} = 0.01$. The temporal dynamics are shown for an environmental variability of $\epsilon = 0.5$ (a) and $\epsilon = 0.2$ (c).

Figure S10: Evolvability per generation

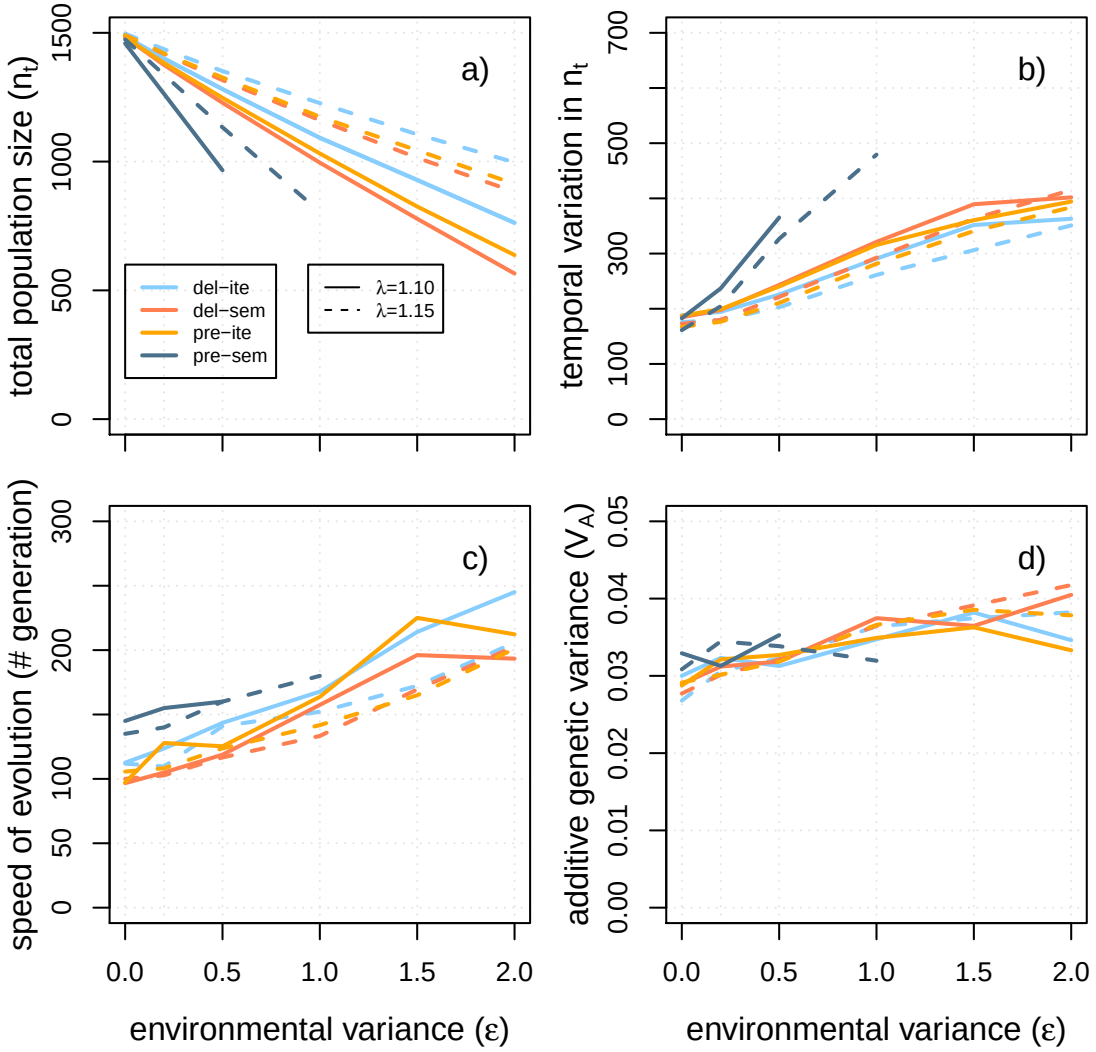

Figure S10: These graphs are identical to Fig. 5, except that the speed of evolution (c) is quantified as the number of generations (not years!) to reach 90% of the novel phenotypic optimum after climate change. For this purpose, the number of years to reach the threshold was divided by the average generation time of each life-history strategy at stable conditions from table 1. Please not that the realized generation time in the course of environmental change might differ from these estimates that have been calculated at equilibrium.

Figure S11: Robustness and evolvability with $\omega^2 = 16$

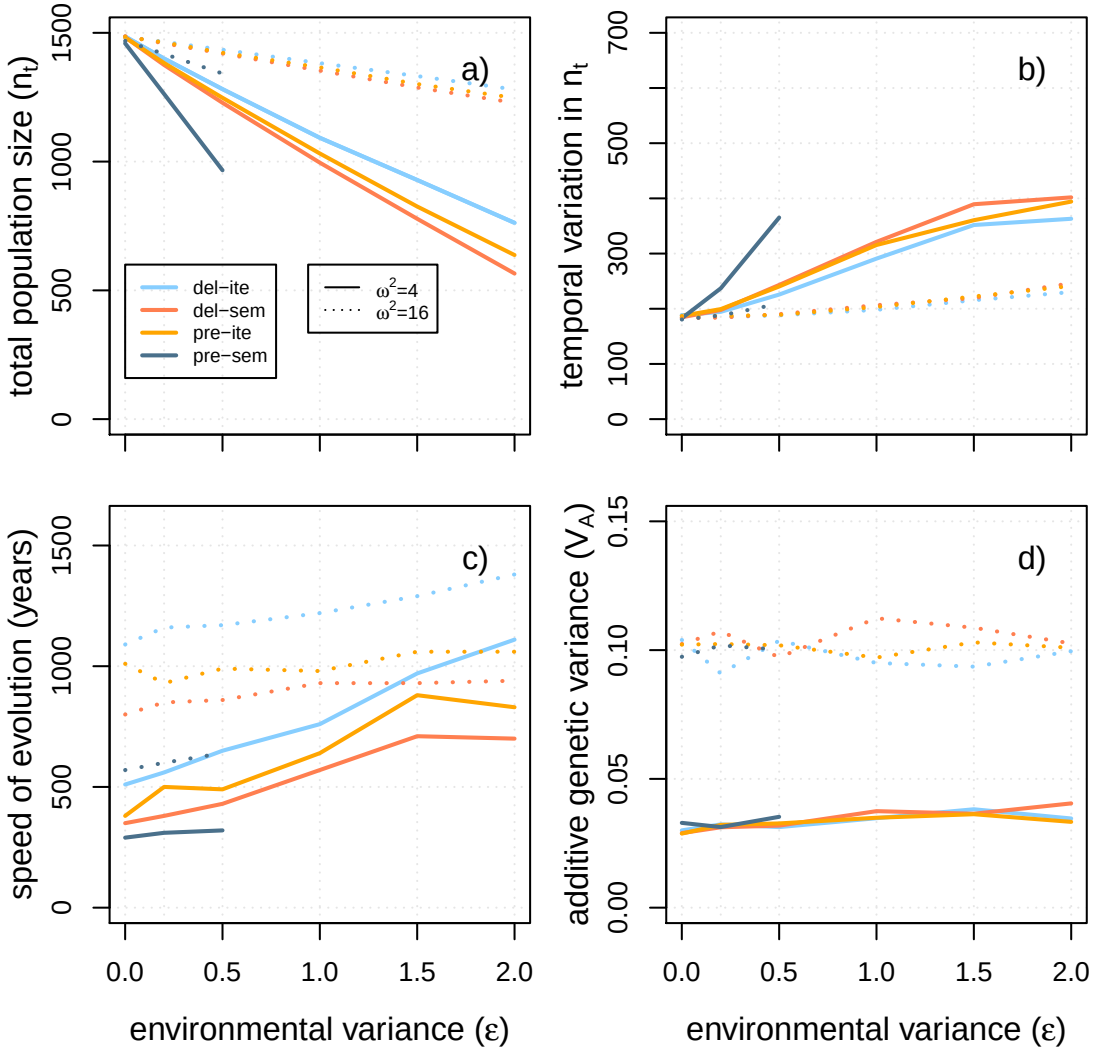

Figure S11: The simulation results for strong selection ($\omega^2 = 4$) are plotted together with the results for weak selection ($\omega^2 = 16$). Weaker selection strength leads to higher population sizes after burn-in (a), lower stochasticity in total population sizes over time (b), a slower speed of evolution (c), and higher levels of additive genetic variance in the juvenile trait (d). However, the rank order of life-history strategies with regard to robustness and evolvability is preserved.

Figure S12: Extinction dynamics with $\omega^2 = 16$

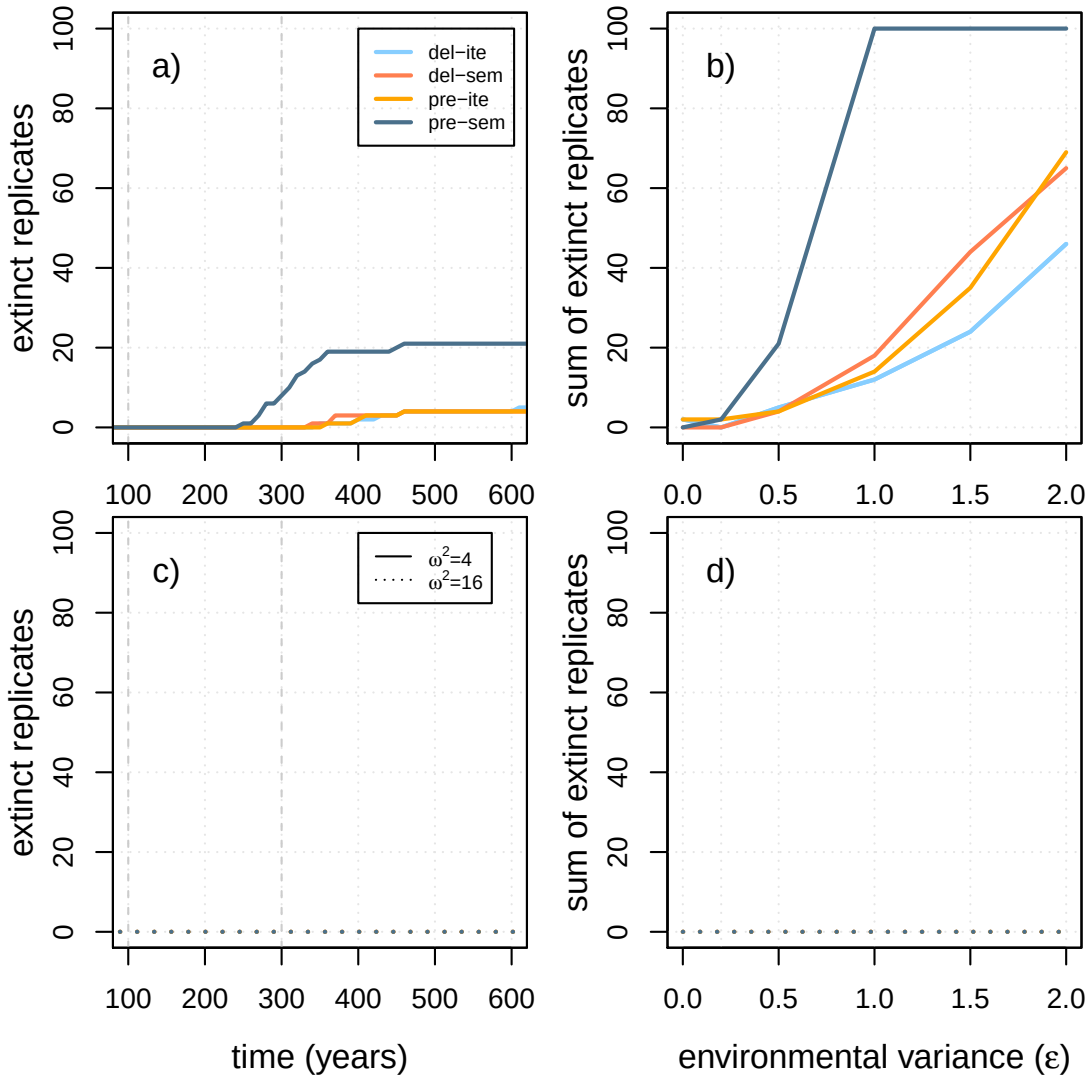

Figure S12: The effects of a stronger ($\omega^2 = 4$, a-b) versus weaker ($\omega^2 = 16$, c-d) selection on extinction probabilities is shown for the environmental change scenario over 200 years, similar to Fig. 6.

Figure S13: Simulated life histories along fast-slow continuum and reproductive strategy

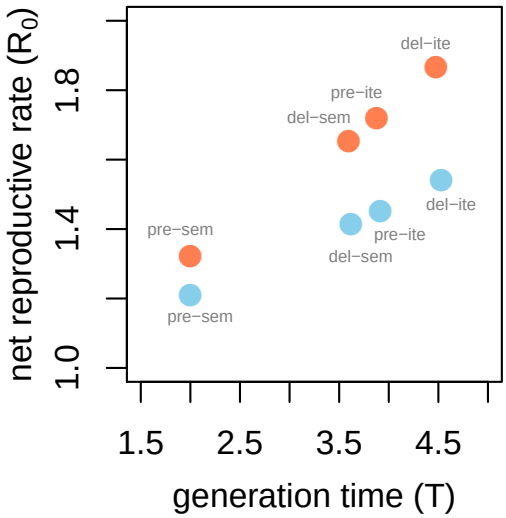

Figure S13: The generation time (T) of each simulated life history is plotted against its net reproductive rate (R_0) from table 1. While the blue circles illustrate life histories standardized for $\lambda_{max} = 1.10$, orange dots represent life histories with $\lambda_{max} = 1.15$. While the x-axis could be interpreted to represent the fast-slow continuum, the y-axis might rather illustrate the reproductive strategy axis as described in meta-analyses (Salguero-Gómez et al., 2017).